PHYSICAL REVIEW B VOLUME 36, NUMBER 10 1 OCTOBER 1987

Domain-wall interactions. II. High-order phases in the axial next-nearest-neighbor Ising model

Michael E. Fisher*
Baker Laboratory, Cornell University, Ithaca, New York 14853

Anthony M. Szpilka†
General Electric Company, Corporate Research and Development, P.O. Box 8, Schenectady, New York 12301

(Received 6 April 1987)

A general formalism recently introduced for the study of physical systems exhibiting uniaxial, spatially modulated commensurate phases is applied to the axial next-nearest-neighbor Ising (ANNNI) model in $d>2$ dimensions with arbitrary interlayer coordination numbers. Asymptotically exact low-temperature expressions for the domain-wall tension, and for the pair, triplet, and higher-order wall-wall interaction potentials characterizing the low-temperature phases, are calculated explicitly by a transfer-matrix method. The wall interaction potentials determine the phase diagram at low temperatures and reveal a new infinite sequence of mixed phases, $\langle 2^k 3 2^{k+1} 3 \rangle$ $(k=1,2,\ldots)$. Some confusing discrepancies in earlier work are resolved and certain approximations are exhibited as limiting cases of the general results. The limit of infinite coordination numbers yields the exact low-temperature *mean-field* phase diagram, which, contrary to some speculations, is seen to be qualitatively correct in the low-temperature limit.

I. INTRODUCTION AND SUMMARY

In a previous paper,[1] hereinafter designated I, we presented a general formalism for the study of physical systems exhibiting uniaxial striped phases, in which homogeneous domains of an underlying ordered phase are separated by an array of parallel, localized walls at successive separations $l_1, l_2, l_3, \cdots$. The basis for this formalism was a rendition of the free-energy density of the system as a sum of domain-wall tensions, $\Sigma(T,\mu,\cdots)$, associated with individual walls, plus pair, triplet, quadruplet, and all higher-order many-wall interaction potentials, $W_n(T,\mu,\cdots;\{l_i\})$, $n\geq 2$, to account for the effective forces exerted by the walls on one another. It was demonstrated in I that the main features of the $(T,\mu,\cdots)$ phase diagram are governed by the functional form of the wall tension and the pair interactions $W_2(l)$ alone, although the triplet, $W_3(l,l')$, and higher-order interactions can lead to a succession of further refinements of the phase diagram which may, in some cases, yield infinite sequences of spatially modulated, commensurate ordered phases.

For models with short-range couplings, asymptotically exact low-temperature expressions for these fundamental domain-wall interactions, W_n, in $d>2$ dimensions can be constructed by a transfer-matrix method, as explained briefly in I. The purpose of the present paper is to carry through this program explicitly for a well-known model that has already been shown to exhibit uniaxial striped phases, namely, the *axial next-nearest-neighbor Ising,* or ANNNI, model. The last paper in this series[2] will describe the results obtained for a distinct model, the *three-state chiral clock,* or CC_3, model. Although the ANNNI and CC_3 phase diagrams possess many similarities, there are also significant differences that directly reflect the different character of the wall interactions in these two models, so illustrating the different types of behavior that may be anticipated in real systems. A brief summary of the main results has been published.[3]

The ANNNI model has by now accumulated a history of applications to various physical systems, as well as numerous theoretical analyses. The model arose originally[4] from attempts to understand spatially modulated magnetic ordering observed in various lanthanide rare-earth metals and in certain alloys. Although Elliott[4] considered only $(n=1)$-component or Ising spins, the suggestion that the complex magnetic ordering could be modeled by spins interacting only through *near-neighbor* couplings was advanced at about the same time by several others, who studied models with $(n=2)$-component or XY spins.[5-9] More recently, the ANNNI model has been adopted in attempts to model complex ordering in ferroelectrics,[10] mineral polytypes,[11] and binary alloys,[12] as well as the structure of chemisorbed gas films[13] and microemulsions.[14] (For recent reviews, see Bak,[15] Selke,[16] or Yeomans.[17])

Although neither the ANNNI model nor its mean-field theory is analytically solvable, many details of its phase diagram in $d>2$ dimensions have already been revealed through (i) Monte Carlo simulations,[18-20] (ii) numerical solutions of the mean-field equations on finite lattices[20-25] or by iteration of a discrete mapping,[26] (iii) analytic solutions of approximations to the mean-field Hamiltonian,[27-29] and (iv) low-temperature series expansions of the exact free energy.[19,30-32] These numerous calculations have revealed a rich variety of phases displaying complicated spatially modulated order.

Of particular interest for the present work, however, is the discovery in several of the earlier calculations that many of these phases at low temperatures can be simply characterized by the particular interwall spacings arising in an elementary uniaxial striped structure.[27-32] Here we determine, without resorting to mean-field or other approximations, which of these possible wall patterns ac-

tually exist as stable phases, using the method developed in I. In this way, we rederive the asymptotically exact low-temperature results of Fisher and Selke[30–32] in a way which eliminates much of the algebraic complexity of their approach and, furthermore, is based on the transparent and physically intuitive notion of interacting domain walls. The present analysis, however, goes beyond these previous calculations, which only revealed the existence of the "simple periodic" striped phases (having a single interwall spacing) $\langle 2^k 3 \rangle$ for $k=0,1,2,\ldots$: here we demonstrate how "mixed" phases (in which two or more different interwall spacings alternate), such as $\langle 2^k 32^{k+1}3 \rangle$, are stabilized by the many-wall interactions $W_{(n\geq 3)}$. These phases are found to exist down to arbitrarily low temperatures, although previously there had been numerical evidence of the existence of mixed phases only at considerably higher temperatures.[24,25]

Furthermore, the transfer-matrix calculations reported here extend the model to arbitrary in-layer and interlayer coordination numbers, q_0, and q_1 and q_2; previously, only $q_1=q_2=2$ had been considered. One reward of this effort is that by taking, appropriately, the limits q_0, q_1, and $q_2\to\infty$, we can deduce the exact low-temperature *mean-field* phase diagram of the ANNNI model. This permits the resolution of an apparent discrepancy between the results of Fisher and Selke, and those of a harmonic approximation to mean-field theory developed by Villain and Gordon.[29,33] We find that, contrary to some speculations,[33] the mean-field theory of the ANNNI model *does* qualitatively reproduce the correct low-temperature phase diagram for finite q_0, q_1, and q_2. It transpires, however, that the same is *not* true for the CC_3 model,[2,3] so that the result is nontrivial.

The layout of this paper is as follows. Section II presents the necessary notation and the general ANNNI Hamiltonian and defines, in this context, the "domains" and "walls." Certain elements of the notation of Fisher and Selke are also recalled and adopted in Sec. II B, both for convenience and in order to facilitate comparison of their approach with the present one: it turns out that the "standard structural coefficients" of their free-energy expansion are closely related to the domain-wall interactions, W_n, as explored in Sec. II C. Section III explains the actual transfer-matrix calculation of the W_n, and derives the resulting phase diagram: see Fig. 4. The original model, as defined on a simple cubic lattice with $q_1=q_2=2$, is treated first, in Secs. III A–III D: then, in Secs. III E and III F the calculations are extended to arbitrary lattice coordination numbers. Some concluding remarks are made in Sec. IV.

II. DEFINITIONS AND FORMALISM

A. Domains and walls at low temperature

The ANNNI model is constructed from a set of commuting Ising spin variables $s_{\mathbf{r}}$ which take the values $+1$ or -1 (also denoted as $\uparrow$ or $\downarrow$, or "up" or "down," respectively) and reside on the sites $\mathbf{r}$ of a d-dimensional lattice. One direction in this lattice (call it the z axis) is singled out: within every $(d-1)$-dimensional lattice "plane" or "layer" *normal* to this axis, there is a spin coupling $J_0(\delta)$ along each nearest-neighbor lattice vector δ. Between adjacent layers, however, there is a coupling $J_1(\delta')$ along every one of a set of equivalent lattice vectors δ' (where the equivalence is with respect to spatial translations); similarly, between next-nearest-neighbor layers, there is a coupling $J_2(\delta'')$ along every one of a set of equivalent lattice vectors δ''. On physical grounds, the vectors δ' and δ'' are usually taken to be the *shortest* vectors between nearest-neighbor and next-nearest-neighbor pairs of layers, respectively, although formally that is not required. If, further, $H_{\mathbf{r}}$ denotes the magnetic field at site $\mathbf{r}$, then the ANNNI Hamiltonian may be written as

$$\mathcal{H}=\sum_{\mathbf{r}}\left[-\sum_{\delta}J_0(\delta)s_{\mathbf{r}}s_{\mathbf{r}+\delta}-\sum_{\delta'}J_1(\delta')s_{\mathbf{r}}s_{\mathbf{r}+\delta'}-\sum_{\delta''}J_2(\delta'')s_{\mathbf{r}}s_{\mathbf{r}+\delta''}-H_{\mathbf{r}}s_{\mathbf{r}}\right]. \tag{2.1}$$

The coordination numbers within a layer, among adjacent layers, and among next-nearest-neighbor layers, will be denoted $q_0\equiv q_\perp$, q_1, and q_2, respectively. Typically, the couplings J_0, J_1, and J_2 are taken to be constants independent of the δ; that assumption will also be made throughout this work, except where a dependence is specifically indicated. Thus, for the commonly considered case of the simple cubic lattice, one has $d=3$, $\delta=\hat{x}$ or $\hat{y}$, $\delta'=\frac{1}{2}\delta''=\hat{z}$, $q_0=4$, and $q_1=q_2=2$.

The remainder of this paper will primarily be concerned with the model in zero field. When $H_{\mathbf{r}}\equiv 0$, it suffices to restrict attention to $J_1(\delta')\geq 0$, since the model is invariant under the mapping $J_1(\delta')\to -J_1(\delta')$ if all spins in every second layer are reversed. It will also be assumed throughout that $J_0(\delta)>0$, corresponding to ferromagnetic in-layer coupling, so that, in the ground state, the spins of each layer will be aligned all $\uparrow$ or all $\downarrow$. To minimize $\mathcal{H}$, then, one need only find the optimum stacking arrangement of these $\uparrow$ and $\downarrow$ layers: in this one-dimensional problem, the sole remaining parameter of relevance is the "competition ratio"

$$\kappa\equiv -q_2J_2/q_1J_1\equiv\tfrac{1}{2}+\delta\ . \tag{2.2}$$

(Here, the minus sign is introduced purely for convenience, and the scalar δ bears no relation to the vector δ.) For $J_2\geq 0$ ($\kappa\leq 0$), it is clear that the ground state is always fully ferromagnetic; for $J_2<0$ ($\kappa>0$), however, a competition arises between the ferromagnetic coupling J_1 which prefers parallel alignment of spins in adjacent layers, and the antiferromagnetic coupling J_2 which prefers antiparallel alignment of spins in next-nearest-neighbor layers. The resulting ground state is easily calculated (see e.g., Selke and Fisher[18,32]): for $\kappa<\frac{1}{2}$ ($\delta<0$), one finds that J_1 dominates and the ground state is ferromagnetic, but for $\kappa>\frac{1}{2}$ ($\delta>0$), it is J_2 which dominates and the ground-state layer sequence is a periodic "two up, two down" pattern ($\cdots\uparrow\uparrow\downarrow\downarrow\uparrow\uparrow\downarrow\downarrow\cdots$). This sequence is conveniently denoted $\langle 2\bar{2}\rangle$ or $\langle 2\rangle$, where, in general,

$\langle j_1\bar{k}_1 j_2\bar{k}_2 \cdots j_n\bar{k}_n \rangle$

represents a periodic layer sequence whose fundamental period consists of j_1 ↑ layers (a "j_1 band"), followed by k_1 ↓ layers (a "$\bar{k}_1$ band"), then a j_2 band, and so on, concluding with a $\bar{k}_n$ band. The abbreviation $\langle 2 \rangle$ for $\langle 2\bar{2} \rangle$ is useful in zero field, where the model is invariant under reversal of all spins: thus, the ferromagnetic phase is denoted simply $\langle \infty \rangle$. *At* the "multiphase point" $\kappa=\frac{1}{2}$ ($\delta=0$) separating the $\langle \infty \rangle$ and $\langle 2 \rangle$ ground states, there occurs an infinite degeneracy, insofar as any layer sequence containing no 1 or $\bar{1}$ bands is a possible ground state.[32] This degeneracy implies a finite zero-temperature entropy per *layer*[34] of $k_B \ln(1+\sqrt{5})/2$; note, however, that the entropy per *spin* is still zero,[32] so that the Third Law of Thermodynamics is not violated. It is the breaking of this multiphase-point degeneracy at nonzero temperatures that leads to the complicated phase diagram of the ANNNI model.

Fisher and Selke developed a systematic low-temperature series expansion of the free energy of the zero-field ANNNI model,[19,30–32] to examine how the infinite ground-state degeneracy at the multiphase point is broken at small positive temperatures. In their scheme, the calculation of the partition function (or, more precisely, of its logarithm, the free energy) is constructed order by order, with the nth-order term arising from all those excited states having n spins flipped from their respective ground-state orientations. From the Hamiltonian (2.1), breaking a single "in-layer" bond is associated with a Boltzmann factor

$$w \equiv e^{-2K_0} \quad \text{with} \quad K_i \equiv J_i/k_B T \quad \text{for } i=0,1,2 \ . \tag{2.3}$$

Hence, overturning one spin in a fully ferromagnetic layer gives rise to a total in-layer Boltzmann factor of

$$w_0 \equiv w^{q_0} \ . \tag{2.4}$$

This is the principal small parameter of the Fisher-Selke expansion: it defines the temperature range over which their approach (and the one we present below) are valid. Provided

$$w_0 \ll 1 \quad (\text{i.e., } k_B T \ll q_0 J_0) \ ,$$

each individual layer retains a nonzero net magnetization (↑ or ↓), and all stable phases can be characterized by their stacking sequence of ↑ and ↓ layers along the axial direction.

The first step of this calculation, which considers only a single flipped spin, is quite easy to carry out. It indicates[32] a wedge of $\langle 3 \rangle$ phase springing from the multiphase point and separating $\langle \infty \rangle$ from $\langle 2 \rangle$, as illustrated in Fig. 1. The width of this $\langle 3 \rangle$ phase along the κ axis at fixed small T is $O(K_1^{-1} w_0)$. *On* the $\langle \infty \rangle$:$\langle 3 \rangle$ boundary, *only* the $\langle \infty \rangle$ and $\langle 3 \rangle$ phases can coexist: any other phase would have a free energy larger by a term of order w_0. Since further terms of the free-energy expansion will arise from excited states with at least two flipped spins and hence be of order w_0^2 or smaller, they cannot overcome this difference. Thus for small w_0 one concludes that the $\langle \infty \rangle$:$\langle 3 \rangle$ boundary marks a stable, first-order transition of the model. [This statement breaks down[35] in the sufficiently *anisotropic* case $x \equiv e^{-2K_1} < w_0$ (i.e., $J_1 > q_0 J_0$), and also at the other extreme, where $1-x \approx 2K_1 < w_0$: in these cases, the new phase $\langle 4 \rangle$ acquires a narrow region of stability between $\langle \infty \rangle$ and $\langle 3 \rangle$.]

On the $\langle 3 \rangle$:$\langle 2 \rangle$ *pseudo*boundary, however, *all layer sequences composed of* 2 *and* 3 *bands only* remain degenerate: this is indicated in Fig. 1 by the dots decorating this boundary. One must proceed to higher orders of the free-energy series expansion in order to resolve this degeneracy, and then any phases found to be stable between $\langle 3 \rangle$ and $\langle 2 \rangle$ must necessarily have widths $K_1 \Delta\kappa = O(w_0^2)$ or less.

This first step of the Fisher-Selke expansion thus establishes that in the vicinity of the $\langle 3 \rangle$:$\langle 2 \rangle$ pseudoboundary at low temperatures, any stable phase can be written in the form

$$\langle 2^{j_1} 3^{k_1} 2^{j_2} 3^{k_2} \cdots 2^{j_m} 3^{k_m} \rangle$$

(where m would be infinite for an aperiodic phase). *Equivalently*, any such phase may be regarded as composed of $\langle 2 \rangle$-phase *domains* separated by 3-band *walls*, where a domain of width k is comprised of k adjacent 2 bands, and a wall consists of a single 3-band. Clearly, in order to retain full generality, $\langle 2 \rangle$-phase domains of zero width must then be allowed. Of course, no reason has been given so far for preferring this description of the possible phases to the alternative which regards them as composed of $\langle 3 \rangle$-*phase* domains separated by 2-*band* walls: our choice of convention is guided by the results of the complete Fisher-Selke expansion[32] and other early work,[27–29] which indicated that the phases in-

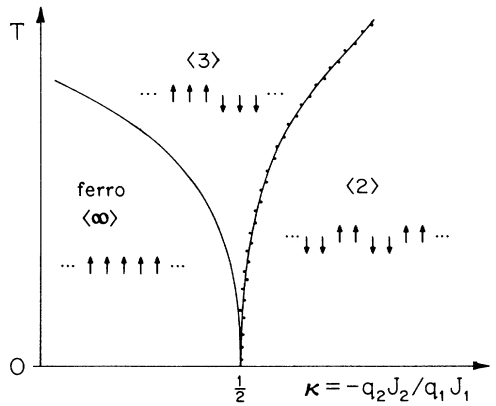

FIG. 1. Schematic phase diagram of the zero-field ($d>2$)-dimensional ANNNI model from a low-temperature series expansion of the free energy to leading order (one-spin-flip excitations). The $\langle \infty \rangle$:$\langle 3 \rangle$ phase boundary, drawn as a solid line, marks a first-order transition, stable against all higher-order excitations (except in certain cases of sufficiently anisotropic spin couplings—see text). The $\langle 3 \rangle$:$\langle 2 \rangle$ *pseudo*boundary, however, shown as a line decorated with dots, may be, and, in this case, *is*, unstable to intermediate phases composed of 2 and 3 bands only.

terpolating between $\langle 3\rangle$ and $\langle 2\rangle$ are of the form $\langle 2^k 3\rangle$, in which 3 bands do indeed occur only singly as "walls." It is important to note, however, that our identification of domains and walls at this point is purely arbitrary and will not influence or restrict the set of phases that we subsequently establish as being stable. In particular, we shall explicitly demonstrate the stability of phases more complicated than just the "simple periodic" $\langle 2^k 3\rangle$ phases.

Given that all stable phases on the $\langle 3\rangle$:$\langle 2\rangle$ pseudoboundary may be characterized as uniaxial "striped" phases, we may now employ the formalism developed in I to obtain further refinements of the phase diagram of Fig. 1. For computational convenience we introduce the reduced free-energy density

$$f \equiv F_N / N k_B T \ , \tag{2.5}$$

where F_N is the total free energy of a lattice of N sites, and the reduced domain wall tension and wall interactions

$$\sigma(T,\kappa) = \Sigma(T,\kappa)/k_B T \ ,$$
$$\overline{W}_n(T,\kappa;l_1,\ldots,l_{n-1}) = W_n(T,\kappa;l_1,\ldots,l_{n-1})/k_B T \ . \tag{2.6}$$

Then the reduced free-energy density may be written exactly in terms of the background free-energy density f_0 of the pure $\langle 2\rangle$ phase and the reduced n-wall interactions $\overline{W}_n$ among the 3-band walls, as

$$f(T,\kappa;\{l_i\}) \equiv f_0(T,\kappa) + \Delta f(T,\kappa;\{l_i\}) \ , \tag{2.7}$$

with the basic decomposition

$$\Delta f(T,\kappa;\{l_i\}) \equiv \lim_{L,\mathcal{N}\to\infty} \frac{1}{L} \sum_{i=1}^{\mathcal{N}} \left[\sigma(T,\kappa) + \sum_{n=2}^{\infty} \overline{W}_n(T,\kappa;l_i,l_{i+1},\ldots,l_{i+n-2}) \right]$$
$$= \lim_{L,\mathcal{N}\to\infty} \frac{1}{L} \left[\mathcal{N}\sigma + \sum_{i=1}^{\mathcal{N}} [\, \overline{W}_2(l_i) + \overline{W}_3(l_i,l_{i+1}) + \cdots] \right] . \tag{2.8}$$

Here $\mathcal{N}$ denotes the number of walls in a system of L layers, and the l_i denote the "axial" distances between successive walls: specifically, if there are k_i 2 bands between the ith and $(i+1)$th 3-band walls, then these two walls are $l_i = 2k_i + 3$ lattice layers apart (with $l_i \geq 3$).

As discussed in I, the phase diagram of the model can now be deduced from the variation of the (reduced) domain wall tension $\sigma(T,\kappa)$ and the functional form and variation of the pair interaction, $\overline{W}_2(T,\kappa;l)$, of the triplet interaction, $\overline{W}_3(T,\kappa;l,l')$, etc. To compute these n-wall interactions, it is convenient at this point to adopt some of the notation introduced by Fisher and Selke;[32] moreover, the use of this notation will facilitate comparison of their approach with the present one and reveal the physical significance of some of their formalism.

B. Free-energy expansion of Fisher and Selke

The reduced free-energy density to be minimized at nonzero temperatures may be written as

$$f(T,\kappa;\{q_i J_i\}) = \beta E_0 - \frac{1}{N} \ln \left[1 + \sum_{n=1}^{\infty} \Delta Z_N^{(n)} \right] , \tag{2.9}$$

where $\beta = 1/k_B T$ and E_0 is the ground-state energy per spin, and $\Delta Z_N^{(n)}$ denotes the partial partition function summed only over those states having n spins flipped from their ground-state orientations, with energies measured relative to E_0. As discussed above, each term in $\Delta Z_N^{(1)}$ contains an in-layer Boltzmann factor $w_0 \equiv w^{q_0}$, each one in $\Delta Z_N^{(2)}$ contains either w^{2q_0} or (if the two spins flipped are in-layer nearest neighbors) w^{2q_0-2}, and, similarly, each term of $\Delta Z_N^{(n)}$ is roughly of order $w^{nq_0} = w_0^n$. Therefore, provided w_0 is much less than unity (i.e., T is near 0), one can treat (2.9) as a series expansion in w. (One sees immediately that such an expansion will *not* work for $d = 2$ dimensions, however, because on, say, a square lattice, where the "layers" are lines, flipping *any number* of in-layer nearest-neighbor spins always yields an in-layer Boltzmann factor of only $w^{q_0} \equiv w^2$.) An important simplifying feature of this expansion is that, according to a linked cluster theorem,[32] all terms in $\Delta Z_N^{(n)}$ involving the second or higher powers of N *cancel* exactly on taking the logarithm in (2.9). (This feature is, of course, necessary to ensure the existence of a regular thermodynamic limit.) As a result, if

$$\Delta Z_N^{(n)} \equiv \xi_1^{(n)} N + \xi_2^{(n)} N^2 + \xi_3^{(n)} N^3 + \cdots \ , \tag{2.10}$$

then f is simply given by

$$f = \beta E_0 - \sum_{n=1}^{\infty} \xi_1^{(n)} \ . \tag{2.11}$$

Consider now the first step of the calculation (one spin flip). The Boltzmann factor associated with the flip depends on the orientations of the nearby layers: since axial couplings extend to second-nearest neighbors, there are (modulo reflections and spin inversion) only five distinct *layer sequences*, μ, in which the spin to be flipped can reside. The associated Boltzmann factors, $e^{-\beta\epsilon_\mu}$, may be written as products of the in-layer Boltzmann factor $w \equiv e^{-2K_0}$ and the "axial" Boltzmann factors

$$x \equiv e^{-2K_1}, \quad x^{\kappa'} \equiv x^{q_1\kappa/q_2} = e^{2K_2} \ . \tag{2.12}$$

To construct the partial partition function $\Delta Z_N^{(1)}$, one must also know the *count*, N_μ, or number of excited states of the lattice containing each of the possible layer

sequences μ, respectively. This count clearly will depend on the particular ground-state layer configuration of the lattice about which one has chosen to expand: that configuration may in turn be characterized by specific values of the single-band "structural variables" ρ_k ($k=1,2,3,\ldots$), which denote the number of k bands per layer.[36] Thus, the necessary counts N_μ are polynomial functions of the $\{\rho_k\}$.

In higher orders of the expansion, where the excited states contain two or more flipped spins, the set of distinct layer sequences μ in which those flipped spins can reside grows more complicated than the five simple sequences mentioned above. Accordingly, the description of their counts, N_μ, can no longer be accomplished by the single-band structural variables $\{\rho_k\}$, but requires more general variables ρ_ν, which denote the number of occurrences per layer in the ground-state configuration of the layer sequence ν. For example, the periodic lattice layer configuration $\langle 232^23\rangle$ leads to the structural variables

$$\begin{aligned}&\rho_2=\tfrac{1}{4},\quad \rho_3=\tfrac{1}{6}\ ,\\ &\rho_{22}=0,\quad \rho_{23}=\rho_{32}=\tfrac{1}{6},\quad \rho_{33}=0\ ,\\ &\rho_{222}=0,\quad \rho_{223}=\tfrac{1}{12},\ \text{etc.}\end{aligned}\tag{2.13}$$

By virtue of the linked-cluster theorem as embodied in (2.10) and (2.11), the free energy f remains, to all orders in w_0, a *linear function* of the $\{\rho_\nu\}$,[32] and may consequently be written as

$$\begin{aligned}f(\{\rho_\nu\};w,x,\delta)&\equiv a_0(w,x;\delta)+\sum_\nu a_\nu(w,x;\delta)\rho_\nu\\ &\equiv a_0+\sum_{n=1}^{\infty}\Delta f^{(n)}\ ,\end{aligned}\tag{2.14}$$

where the nth-order contribution (n spins flipped) to the free energy is

$$\Delta f^{(n)}(\{\rho_\nu\};w,x,\delta)\equiv\sum_\nu a_\nu^{(n)}(w,x;\delta)\rho_\nu\ .\tag{2.15}$$

Assuming one can compute the coefficients $a_\nu^{(n)}$ here, the actual values to be assigned to the ρ_ν would then be those that minimize f: those values of $\{\rho_\nu\}$ would in turn characterize (in practice, uniquely) the layer sequence of the stable phase, as in the example (2.13) for $\langle 232^23\rangle$. The minimization of f over the $\{\rho_\nu\}$ at each order constitutes a linear programming problem, *provided* f has been expressed as a function only of a subset of the $\{\rho_\nu\}$ which are *linearly independent* and hence represent "standard" structural variables.[32] Indeed, the standard structural variables, by their definition and construction, satisfy various linear inequalities which serve to define the linear programming problem.

In the study of the $\langle 3\rangle$:$\langle 2\rangle$ pseudoboundary, the dependency relations among the $\{\rho_\nu\}$ are easily identified. If ν denotes a sequence of length m bands, then longer sequences of length $m+1$ or $m+2$ bands which contain ν can be formed only by adding 2 or 3 bands before or after it, so one has[32]

$$\begin{aligned}&\rho_\nu=\rho_{2\nu}+\rho_{3\nu}=\rho_{\nu 2}+\rho_{\nu 3}\ ,\\ &\rho_{2\nu}=\rho_{2\nu 2}+\rho_{2\nu 3},\quad \rho_{\nu 2}=\rho_{2\nu 2}+\rho_{3\nu 2}\ ,\\ &\rho_{3\nu}=\rho_{3\nu 2}+\rho_{3\nu 3},\quad \rho_{\nu 3}=\rho_{2\nu 3}+\rho_{3\nu 3}\ .\end{aligned}\tag{2.16}$$

Hence, given any *one* of the set of the four structural variables $\{\rho_{2\nu 2},\rho_{2\nu 3},\rho_{3\nu 2},\rho_{3\nu 3}\}$ for sequences of length $m+2$ bands, one can express the other three variables in terms of it and the structural variables for shorter sequences. The choice of the one independent or standard structural variable from the set is of course arbitrary, but the following convention will prove the most convenient for the layer configurations encountered hereafter.[37]

Let the standard structural variable for length $m+2$ based on a "core" sequence ν of length m bands be $\rho_{3\nu 3}$. The first few standard structural variables are thus

$$\begin{aligned}&\rho_3\ (m=1);\quad \rho_{33}\ (m=2);\quad \rho_{323},\ \rho_{333}\ (m=3)\ ;\\ &\rho_{3223},\ \rho_{3233},\ \rho_{3323},\ \rho_{3333}\quad (m=4)\ .\end{aligned}\tag{2.17}$$

By rewriting the free energy in terms of a set of standard structural variables ρ_ν as in (2.14) and (2.15), the Fisher-Selke approach thus transforms the problem of calculating f into that of computing the standard structural *coefficients*, a_ν. At this point, these coefficients have no apparent physical significance but we shall now show that they are intimately related to the n-wall interactions, W_n, among the 3-band walls.

C. Relation of domain-wall interactions to structural coefficients

To relate the domain wall interactions W_n to the standard structural coefficients a_ν, consider first the single-wall tension σ in (2.8). As discussed in I, this is given by the reduced free-energy difference

$$\sigma(T,\kappa)\equiv\Sigma(T,\kappa)/k_BT=\lim_{L\to\infty}L\,(f[C]-f_0)\ ,\tag{2.18}$$

where the configuration C consists of a single 3-band wall within an otherwise homogeneous $\langle 2\rangle$ background phase (whose free energy is f_0). In the Fisher-Selke procedure, these reduced free-energy densities $f[C]$ and f_0 are given by (2.14), where the sum runs only over those "standard" sequences ν constructed according to the convention stated above (2.17). Since ρ_ν denotes the number of occurrences per layer of the layer sequence ν in the given configuration, then for the pure background $\langle 2\rangle$ phase, having no 3-band walls, all ρ_ν vanish [see (2.17)], whence one simply has

$$f_0=a_0\tag{2.19}$$

in (2.18). In the configuration C, the only nonzero ρ_ν is ρ_3, which evidently assumes the value $1/L$. Thus (2.18) yields

$$\sigma(T,\kappa)=a_3\ .\tag{2.20}$$

An expression for this coefficient a_3, exact through order w_0, can be obtained from the one-spin-flip calculation of $a_2^{(1)}$ by Fisher and Selke[32] [see their Eq. (4.7)], by ap-

pealing to the sum rule $2\rho_2+3\rho_3=1$ which holds near the $\langle 3\rangle$:$\langle 2\rangle$ pseudoboundary (since no other bands are allowed at low T). One thus has

$$\sigma(T,\kappa)=a_3=\tfrac{3}{2}a_2^{(1)}+O(w_0^2)$$
$$=2K_1(\delta-\delta_2^{(1)})+O(w^{2q_0-2}) , \qquad (2.21)$$

where the explicit formula

$$K_1\delta_2^{(1)}(w,x)\equiv(2/q_1)w_0(1-x^{q_1/2})^2(1+\tfrac{1}{2}x^{q_1/2}) \qquad (2.22)$$

specifies the locus of the $\langle 3\rangle$:$\langle 2\rangle$ pseudoboundary in the $(\kappa\equiv\frac{1}{2}+\delta, T)$ plane; see Fig. 1. The surface tension σ therefore exhibits the canonical behavior discussed in I, by vanishing on the boundary which separates the $\langle 2\rangle$ phase with no walls from the $\langle 3\rangle$ phase with walls packed as densely as possible.

The two-wall interaction $\overline{W}_2(l)$ can be similarly expressed in terms of the a_ν. Recall from I that it is defined by

$$\overline{W}_2(T,\kappa;l)=\lim_{L\to\infty} L\Delta f[C(l)]-2\sigma , \qquad (2.23)$$

where the configuration $C(l)$ consists of two 3-band walls at separation l within an otherwise homogeneous background $\langle 2\rangle$ phase. [Recall that our convention in (2.8) takes $l=2k+3$, where k is the number of 2 bands between the two walls.] Since each standard sequence ν begins and ends with a 3 band [recall (2.17)], the only nonzero ρ_ν in $C(2k+3)$ are those with $\nu=3$ (for which $\rho_\nu=2/L$) and $\nu=32^k3$ (for which $\rho_\nu=1/L$). Thus, (2.23) becomes

$$\overline{W}_2(2k+3)=(2a_3+a_{32^k3})-2\sigma=(32^k3) , \qquad (2.24)$$

where we have used (2.20) for σ and introduced the convenient abbreviation

$$a_\nu\equiv(\nu) . \qquad (2.25)$$

By similar reasoning, one readily arrives at the general form for $\overline{W}_n$. Recall from I the definition [analogous to (2.23)]

$$\overline{W}_n(l_1,l_2,\ldots,l_{n-1})\equiv\lim_{L,k_n\to\infty} L\Delta f(\langle 32^{k_1}32^{k_2}\cdots 32^{k_{n-1}}32^{k_n}\rangle)-n\sigma-\sum_{m=2}^{n-1}\sum_{i=1}^{n+1-m}\overline{W}_m(l_i,l_{i+1},\ldots,l_{i+m-2}) , \qquad (2.26)$$

with $l_i=2k_i+3$. Again, according to our convention above (2.17), all standard sequences ν with nonzero ρ_ν in Δf must be of the form

$$32^{k_i}32^{k_{i+1}}\cdots 32^{k_{i+j}}3 ,$$

in addition to the single-band sequence $\nu=3$ itself. By induction, it is immediately apparent that only the longest of these sequences survives the subtractions in (2.26), so that, for all $n\geq 2$,

$$\overline{W}_n(l_1,l_2,\ldots,l_{n-1})=(32^{k_1}32^{k_2}\cdots 32^{k_{n-1}}3) . \qquad (2.27)$$

Thus we conclude that the standard structural coefficients $a_\nu\equiv(\nu)$, suitably defined,[37] are none other than the wall interaction potentials $\overline{W}_n$ entering the basic free-energy decomposition (2.8). As a consequence, note that the various relations among the wall potentials, like

$$\overline{W}_3(l_1,l_2)=\overline{W}_3(l_2,l_1) , \qquad (2.28)$$

which arise from the ANNNI model's symmetry with respect to reflection in any lattice layer, imply corresponding identities among the a_ν.

III. THE DOMAIN-WALL POTENTIALS AND THE PHASE DIAGRAM

In order to refine the phase diagram of Fig. 1 within the crossover regime of width $O(w_0^2)$ about the $\langle 3\rangle$:$\langle 2\rangle$ pseudoboundary (2.22), one must, according to Sec. IV of I, calculate the domain-wall interactions

$$\overline{W}_2(l)=(32^k3) \quad (l=2k+3) , \qquad (3.1)$$

$$\overline{W}_3(l,l)=(32^k32^k3) , \qquad (3.2)$$

and so on, where we have recalled the equivalences to the standard structural coefficients $(\nu)\equiv a_\nu$ from (2.24) and (2.27). This we shall now undertake on the basis of a transfer-matrix method. The transfer matrix $\mathbf{V}(T,\kappa)\equiv\mathbf{V}(w,x)$ serves to generate in a systematic way the leading low-temperature diagrammatic contributions to the potentials, $\overline{W}_n$. The appropriate diagrams and the weights and *signs* with which they enter were analyzed by Fisher and Selke (FS).[32] Accordingly, we start, in Sec. III A, by reviewing the basic results established by FS on which we build. The transfer-matrix calculations begin, in Secs. III B–III D, with the simplest case of axial coordination numbers $q_1=q_2=2$ (as considered by FS). Here we find, to leading order in temperature, that $\mathbf{V}$ may be taken as a 2×2 matrix, $\mathbf{V}_0$. The low-temperature phase diagram found by FS,[30,32] with infinitely many phases, $\langle 2^k3\rangle$ $(k=0,1,2,\ldots)$, is then recovered; see Fig. 2. The matrix $\mathbf{V}_0$, however, displays a *degeneracy* which is broken by the inclusion of higher-order diagrammatic terms that enlarge $\mathbf{V}_0$ into a 4×4 matrix, $\mathbf{V}_1$. The breaking of this degeneracy reveals that at *fixed* low temperature, $T>0$, the ANNNI model actually exhibits a "harmless staircase" or case B behavior, in the notation of I. This is in contrast to a quasicontinuous transition to the $\langle 2\rangle$ phase, with a "devil's last step" or case A behavior, as is, at first sight, suggested by Fig. 2. The point, in a nutshell, is that each boundary $\langle 2^k3\rangle$:$\langle 2^{k+1}3\rangle$ in the FS diagram represents a stable first-order boundary at sufficiently low temperature, thus ensuring the stability of infinitely many discrete phases in the vicinity of the multiphase point. However, "sufficiently low" turns out to entail, as we show here, $T<T_k^0$, where $T_k^0\to 0$ as $k\to\infty$! For $T>T_k^0$

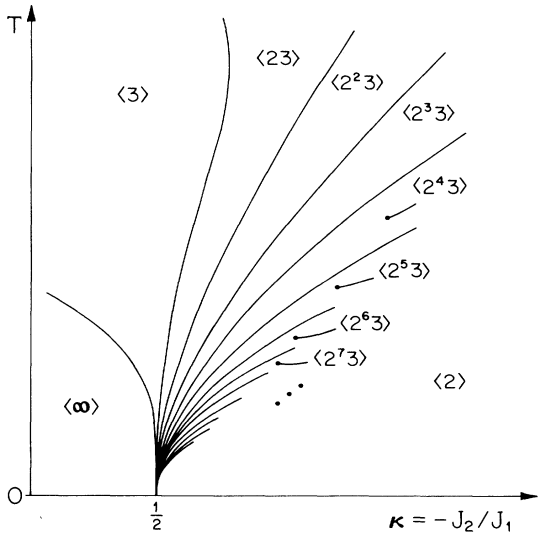

FIG. 2. Sketch of the phase diagram of the $(d>2)$-dimensional ANNNI model near the multiphase point, for $q_1=q_2=2$, following from the analytic low-temperature calculations of Fisher and Selke (Ref. 31). All phases $\langle 2^k3\rangle$ for $k=0,1,2,\ldots,$ are encountered between the ferromagnetic and $\langle 2\rangle$ phases sufficiently close to the multiphase point $(T=0, \kappa=\frac{1}{2})$. All phase boundaries $\langle 2^k3\rangle$:$\langle 2^{k+1}3\rangle$ are of first order at low enough T, but that character is established only up to a bound, T_k^0, which vanishes as $k\to\infty$. No phases beyond the infinite $\langle 2^k3\rangle$ sequence are predicted by the calculations.

the boundary $\langle 2^k3\rangle$:$\langle 2^{k+1}3\rangle$ is only a pseudoboundary and, in fact, is unstable, opening to admit a narrow region of the *mixed phase* $\langle 2^k32^{k+1}3\rangle$. The resulting phase diagram, valid now for any fixed low T (*independent* of k), is shown in Fig. 4, below.[3]

In Sec. III E we go on to show how the principal findings for $q_1=q_2=2$ can alternatively be deduced from an appropriately *modified* 2×2 matrix formalism. By generalizing that formalism to arbitrary q_1 and q_2 (in Sec. III F) we demonstrate that the ANNNI model does *not* exhibit any qualitative change of behavior as the axial coordination numbers q_1 and q_2 increase, even in the full mean-field limit $q_0, q_1, q_2\to\infty$. In fact, the asymptotically exact low-temperature mean-field phase diagram which we obtain for the ANNNI model agrees quantitatively with that deduced by Villain and Gordon[29] from a harmonic approximation to mean-field theory, even though their calculation can be justified only for a model with highly anisotropic spin couplings in the "intermediate" temperature regime[3]

$$q_0J_0 \gg k_BT \gg q_2\,|J_2| \equiv \kappa q_1 J_1 \ . \tag{3.3}$$

The calculations of the $\overline{W}_n$ we now describe are, of necessity, fairly technical: the reader uninterested in the details might skip Sec. III A and advance directly to the leading-order results, (3.19) and (3.22), for $\overline{W}_2(l)$ and $\overline{W}_3(l,l)$.

A. Analysis of the structural coefficients

The leading low-temperature term of the standard structural coefficient (32^k3), needed in (3.1), is determined by the lowest-order excited states of the lattice whose counts involve a nonzero value of ρ_{32^k3}. As discussed in Sec. VI of I, these states must obviously possess a cluster of flipped spins, linked to one another by the couplings J_i, which extend across or "span" a layer sequence at least as long as 32^k3. Since axial couplings extend to second-nearest neighbors, one state with the fewest flipped spins satisfying this requirement is a "chain" along the z axis, having every *second* spin flipped and spanning 32^k3. We can represent this excited state by the symbol

$$|\,s\hat{s}s\,|\underbrace{\hat{s}s\,|\,\hat{s}s\,|\,\hat{s}s\,|\,\hat{s}s\,|\,\cdots\,|\,\hat{s}s}_{k\ \text{2-bands}}\,|\,\hat{s}ss\,|\ . \tag{3.4}$$

Here, each s denotes the orientation of an entire layer ($s=\uparrow$ or $\downarrow$), so that a string of s's represents a band of layers with parallel magnetizations: band edges are denoted by vertical bars. An s marked with a circumflex, $\hat{s}$, indicates that a single spin has been flipped in that layer. The in-layer Boltzmann factor of this state (3.4) is w_0^{k+2}, which, by comparing (2.11) with (2.14), is seen to contribute *negatively* to (32^k3). This result establishes that $(32^k3)=O(w_0^{k+2})$ for all $k\geq0$.

In addition to (3.4), one must sum over all similar chains with the same number of flipped spins in order to obtain the complete leading term of (32^k3). This summation is governed by two rules identified by FS (Ref. 32) which we summarize briefly here.

Let $\nu'\equiv2^k$ denote the "core" of 32^k3 (i.e., the sequence obtained from 32^k3 by removing its first and last bands). By virtue of the relations (2.16), the standard structural coefficient ρ_{32^k3} also appears in the counts N_μ of any excited states involving the (nonstandard) sequences $2\nu'2$, $2\nu'3$, and $3\nu'2$. Since these three sequences can support chains of $k+2$ flipped spins, similar to (3.4), they too will contribute to (32^k3) at leading order w_0^{k+2}. From (2.16), one has

$$\begin{aligned}&\rho_{2\nu'2}=\rho_{2\nu'}-\rho_{\nu'3}+\rho_{32^k3}\ ,\\ &\rho_{2\nu'3}=\rho_{\nu'3}-\rho_{32^k3},\quad \rho_{3\nu'2}=\rho_{3\nu'}-\rho_{32^k3}\ .\end{aligned} \tag{3.5}$$

Since, as noted above, the Boltzmann factor of the standard sequence 32^k3 is to be counted negatively in (32^k3), it follows that the contributions of these nonstandard sequences to (32^k3) are equal to their Boltzmann factors times the extra *signs* given by:

Rule 1: The sequences $2\nu'2$ and $3\nu'3$ contribute negatively to $a_{32^k3}\equiv(32^k3)$, but $2\nu'3$ and $3\nu'2$ contribute positively.

A further set of contributions to (32^k3) at leading order comes from *disconnected* excited states (those containing two or more noninteracting clusters of flipped spins) which, when "collapsed," can yield one of the four sequences of Rule 1. For example, the disconnected configuration μ consisting of the two separated spin flips $|\,s\hat{s}\,|$ and $|\,\hat{s}\hat{s}\,|$ has a count $N_\mu=(N\rho_2)(N\rho_3)-N\rho_{23}$,

where $-N\rho_{23}$, the "excluded volume" term, is needed to subtract from $(N\rho_2)(N\rho_3)$ the number of "collapsed" states, $|\,s\hat{s}\,|\,s\hat{s}s\,|$, in which the two flipped spins interact (thereby giving rise to a total Boltzmann factor different from that of μ.) Hence, μ would contribute to a_{33}: but note the extra minus sign introduced by the decomposition. Now, a chain with $k+2$ flipped spins can be decomposed into disconnected states having 2,3, . . . , or $k+2$ separated segments. A little reflection on the above example reveals that the excluded volume contribution to (32^k3) of each such decomposition is equal to the Boltzmann factor of the disconnected state times an extra sign given by:

Rule 2: A decomposition into p segments of one of the sequences listed in Rule 1 contributes to (32^k3) with a sign of $(-1)^{p-1}$.

One therefore obtains the leading term of (32^k3) by summing the total Boltzmann factors of all chains of $k+2$ flipped spins spanning the sequences governed by Rules 1 and 2. Note that there is some freedom available in the placement of the flipped spins: Adopting for convenience in the remainder of this subsection the simplest case of axial coordination numbers $q_1=q_2=2$, we see from the definitions (2.12) that (3.4) has Boltzmann factor $x^2w_0^{k+2}$, whereas other possible chains spanning 32^k3 and having the same Boltzmann factor are

$$|\,ss\hat{s}\,|\,s\hat{s}\,|\,s\hat{s}\,|\,s\hat{s}\,|\,s\hat{s}\,|\,\cdots\,|\,s\hat{s}\,|\,s\hat{s}s\,| \tag{3.6}$$

and

$$|\,ss\hat{s}\,|\,s\hat{s}\,|\,\hat{s}s\,|\,\hat{s}s\,|\,\hat{s}s\,|\,\cdots\,|\,\hat{s}s\,|\,\hat{s}ss\,|\ . \tag{3.7}$$

In the last example, however, notice that the "defect," "kink," or "soliton," $s\hat{s}\,|\,\hat{s}s$, where two flipped spins are nearest neighbors instead of next-nearest neighbors, could occur at any of the $k+1$ interior band edges.

At first glance, one might suppose that a *next-to-leading* excited state contributing to (32^k3) would be formed by adding to, say, (3.4) an extra flipped spin which is an *in-plane* nearest-neighbor to one of the flipped spins of the chain, namely,

$$|\,s\hat{s}s\,|\,\hat{s}s\,|\,\hat{s}s\,\Big|\begin{matrix}\hat{s}\\ \hat{s}s\end{matrix}\,|\,\hat{s}s\,|\,\cdots\,|\,\hat{s}s\,|\,\hat{s}ss\,|\ , \tag{3.8}$$

where the notation introduced in (3.4) has been generalized in an obvious manner. The extra flipped spin introduces an extra in-layer Boltzmann factor of w^{q_0-2} (not w^{q_0}), as well as an axial factor of $x^{2\kappa}$. Since it could be adjacent to any of the $k+2$ flipped spins of the chain, it follows that the total contribution of all such states to (32^k3) is reduced from the leading term by a factor of order $kx^{2\kappa}w^{q_0-2}$. Actually, however, in the limit $k\to\infty$ with $T>0$ fixed, it transpires that the leading correction is given not by states like (3.8), but by states having an extra spin flipped *in the chain.* It might seem that such states would be formed from (3.4) as, say,

$$|\,s\hat{s}s\,|\,\hat{s}s\,|\,\hat{s}\hat{s}\,|\,\hat{s}s\,|\,\hat{s}s\,|\,\cdots\,|\,\hat{s}s\,|\,\hat{s}ss\,| \tag{3.9}$$

(note the $\hat{s}\hat{s}$ pair), and hence be reduced from the leading term by a factor of order $kx^{2\kappa}w^{q_0}$, which is much less than the factor $kx^{2\kappa}w^{q_0-2}$ associated with (3.8). However, one must recognize that (3.9) contains a "bound pair" of defects, $s\,|\,\underbrace{\hat{s}\hat{s}}\,|\,\hat{s}s\,|$, which can unbind to form a state like

$$|\,s\hat{s}s\,|\,\underbrace{\hat{s}\hat{s}}\,|\,s\hat{s}\,|\,s\underbrace{\hat{s}}\,|\,\hat{s}s\,|\,\cdots\,|\,\hat{s}s\,|\,\hat{s}ss\,| \tag{3.10}$$

with separated defects. Such a state has just as many flipped spins as (3.9), but now *each* defect has the freedom to occupy roughly k positions, so the total contribution of such states to (32^k3) is reduced from the leading term by a factor of order $k^2x^{4\kappa}w^{q_0}$. For sufficiently large k and fixed $T>0$ this dominates the factor $kx^{2\kappa}w^{q_0-2}$ associated with (3.8).

Finally, for the sake of completeness, we mention the one other type of excited state that contributes to (32^k3), which may not be obvious. That is what might be called a "doubly flipped spin," which can arise from the *superposition* of two parts of a *disconnected* configuration. For example, the disconnected configuration μ consisting of the two separated chains $|\,s\hat{s}s\,|\,\hat{s}s\,|\,\hat{s}s\,|$ and $|\,\hat{s}s\,|\,\hat{s}s\,|\,\hat{s}ss\,|$ contributes to (32^33) through the excluded volume term associated with

$$|\,s\hat{s}s\,|\,\hat{s}s\,|\,\ddot{s}s\,|\,\hat{s}s\,|\,\hat{s}ss\,|\ , \tag{3.11}$$

where the umlaut denotes a superposition of two flipped spins. Such "doubly flipped spins" *cannot,* however, be separated like the pair of defects in (3.9). Hence, the total contribution to (32^k3) of all such chains containing doubly flipped spins is reduced from the leading term by a factor of order $kx^{2\kappa}w^{q_0}$, which is negligible compared to either the factor $k^2x^{4\kappa}w^{q_0}$ associated with (3.10), or to $kx^{2\kappa}w^{q_0-2}$ associated with (3.8).

B. Lowest-order transfer-matrix results

From the examples in (3.4) and (3.6) and (3.7), one sees that each of the lowest-order chains, with exactly $k+2$ flipped spins spanning one of the four layer sequences $2\nu'2$, $2\nu'3$, $3\nu'2$, or $3\nu'3$ ($\nu'\equiv 2^k$), has only *one* spin flipped in *each* band. It is therefore convenient to imagine constructing the chain by successively adding to its *left* end a single 2 band with one flipped spin. We choose to add bands on the left in order to obtain a closer correspondence with standard matrix notation: for the same reason we will count bands $m=1,2,\ldots$ starting on the *right.* Note that each newly added 2 band (label it m) interacts only with its nearest-neighbor 2 band, $m-1$, to the right. Of course, the spin flipped within band m may reside in either its first (left) or second (right) layer, and similarly for band $m-1$: let these two possible configurations of each band be called states 1 and 2, respectively. In this way, one is led to associate a 2×2 matrix with the transfer operator $\tilde{\mathbf{V}}$ which adds band m to the chain. The (i,j) entry of this matrix, $\tilde{V}_{ij}$, will be taken to describe the case where the flipping of spins has promoted band m to state i and band $m-1$ to state j. The value of $\tilde{V}_{ij}$ is then the total Boltzmann factor, *relative to the ground state,* for all the bonds broken *within* band m and *between* bands m and $m-1$.

[This must, of course, include the standard factor $w_0 \equiv w^{q_0}$ to account for the *in-layer* broken bonds in band m; however, it is convenient explicitly to factor w_0 out of $\tilde{\mathbf{V}}$; see (3.12) below.]

To illustrate this definition, consider the element $\tilde{V}_{11}$, which describes the situation $\hat{s}s \mid \hat{s}s \mid \cdots$. Henceforth, through Sec. III D, we restrict our attention to the simplest case of axial coordination numbers $q_1 = q_2 = 2$: in that case, the chain is perfectly straight. According to the Boltzmann factors defined in (2.12), one has $\tilde{V}_{11} = x \times x^{-1} = 1$, where the factors x and x^{-1} account, respectively, for the broken nearest neighbor bonds between layers 1 and 2 of band m, and between layer 2 of band m and layer 1 of band $m-1$. In similar fashion one obtains the remaining elements of the matrix

$$w_0 \tilde{\mathbf{V}} = w_0 \begin{bmatrix} 1 & x^{1+2\kappa} \\ x^{1+2\kappa} & 1 \end{bmatrix} . \tag{3.12}$$

In constructing and checking this and other matrices below, it is helpful to refer to Table I, which lists, for all possible combinations of flipped and unflipped spins, the Boltzmann factors of the broken nearest neighbor and next-nearest-neighbor axial bonds emanating from the *leftmost* spin and extending to its right.

The partial partition function associated with adding $k+1$ 2 bands to the chain, properly summed over the two possible states of each band, is clearly given by the matrix product $(w_0 \tilde{\mathbf{V}})^{k+1}$. [Note that we consider adding $k+1$ 2 bands since, from the point of view of interactions with flipped spins to its right, the addition of a leftmost, or terminal 3 band after k 2 bands is equivalent to adding on a $(k+1)$th 2 band. The effects due to the actual terminations of the sequence of bands will be accounted for by the vectors defined in (3.15) and (3.16) below.] One must note, however, that not every state generated by the powers of $w_0 \tilde{\mathbf{V}}_0$ should contribute to the coefficient $(32^k 3)$. In particular, there should be no contribution from chains having some band m in state 1 and the adjacent band $m-1$ in state 2, since in that case the two flipped spins are third-nearest neighbors and so are not linked by any bond. This is equivalent to saying that the matrix element $\tilde{V}_{12}$ should be 0. That change is automatically brought about by the subtraction which results from accounting for all the *disconnected* chains as required by Rule 2 above. To incorporate Rule 2 into this transfer-matrix formalism, note that a chain can be disconnected between any two flipped spins (which here means between any two bands), and each such decomposition carries an extra factor of -1. Therefore, one can account for a decomposition between, say, two bands both in state 1, $(\hat{s}s \mid \hat{s}s)$, by *subtracting* from the transfer operator element $\tilde{V}_{11} = \tilde{V}(\underline{\hat{s}_m s_m} \mid \hat{s}_{m-1} s_{m-1})$, which adds $\hat{s}_m s_m$ to the chain, the element

$$\tilde{V}(\underline{\hat{s}_m s_m} \mid s_{m-1} s_{m-1} \cdots \underline{s_m s_m} \mid \hat{s}_{m-1} s_{m-1})$$

associated with adding the underlined bands: the argument of this latter element is meant to indicate that it accounts for the two *interior ends* of the two subchains that result when the chain constructed by $\tilde{V}_{11}$ is disconnected between bands m and $m-1$. To include all possible decompositions, one should then replace $w_0 \tilde{\mathbf{V}}$ by

$$\begin{aligned} w_0 \mathbf{V}_0 &= w_0 \begin{bmatrix} (\underline{\hat{s}s} \mid \hat{s}s) - (\underline{\hat{s}s} \mid ss \cdots \underline{ss} \mid \hat{s}s) & (\underline{\hat{s}s} \mid s\hat{s}) - (\underline{\hat{s}s} \mid ss \cdots \underline{ss} \mid s\hat{s}) \\ (\underline{s\hat{s}} \mid \hat{s}s) - (\underline{s\hat{s}} \mid ss \cdots \underline{ss} \mid \hat{s}s) & (\underline{s\hat{s}} \mid s\hat{s}) - (\underline{s\hat{s}} \mid ss \cdots \underline{ss} \mid s\hat{s}) \end{bmatrix} \\ &= w_0 \begin{bmatrix} \lambda_0 & 0 \\ -x^{2\kappa-1}(1-x^2) & \lambda_0 \end{bmatrix} , \end{aligned} \tag{3.13}$$

where one finds

$$\lambda_0 \equiv 1 - x^{2\kappa} . \tag{3.14}$$

In the first line of (3.13), the band being added to the left end of the chain has been identified by an underbar.

Now the matrix product $(w_0 \mathbf{V}_0)^{k+1}$ correctly sums over all connected and disconnected states of the chain contributing to $\overline{W}_2(l) = (32^k 3)$. It remains only to account for the broken bonds beyond the endmost bands, by pre- and post-multiplying $(w_0 \mathbf{V}_0)^{k+1}$ by appropriate row and column vectors, respectively. Since all four of the layer sequences 2^{k+2}, $2^{k+1}3$, 32^{k+1}, and $32^k 3$ contribute to $(32^k 3)$, each endmost flipped spin may lie within either a 2 or a 3 band. On enumerating all possibilities the needed vectors are then found to be

$$\begin{aligned} \mathbf{b}_0^\dagger &= [\underline{ss} \mid \hat{s}s \mid , \underline{ss} \mid s\hat{s} \mid] = [x^{\kappa-1}, x^\kappa] , \\ \mathbf{c}_0^\dagger &= [\underline{s \mid s\hat{s}s} \mid , \underline{s \mid ss\hat{s}} \mid] = [x^{\kappa+1}, x^{-\kappa}] , \end{aligned} \tag{3.15}$$

and

$$\begin{aligned} w_0 \mathbf{b}_1 &= w_0 \begin{bmatrix} \mid \underline{\hat{s}s} \mid ss \\ \mid \underline{s\hat{s}} \mid ss \end{bmatrix} = w_0 \begin{bmatrix} x^{\kappa+1} \\ x^\kappa \end{bmatrix} , \\ w_0 \mathbf{c}_1 &= w_0 \begin{bmatrix} \mid \underline{\hat{s}s}s \mid s \\ \mid \underline{s\hat{s}}s \mid s \end{bmatrix} = w_0 \begin{bmatrix} x^{1-\kappa} \\ x^{\kappa+2} \end{bmatrix} . \end{aligned} \tag{3.16}$$

(Here the spins being added to the chain have again been underlined.) On summing the contributions of the four layer sequences with signs as given by Rule 1 and using (3.1), one concludes

$$\begin{aligned} \overline{W}_2(2k+3) = (\mathbf{c}_0^\dagger - \mathbf{b}_0^\dagger) \mathbf{V}_0^{k+1} (\mathbf{b}_1 - \mathbf{c}_1) w_0^{k+2} \\ \times [1 + O(k^2 x^{4\kappa} w^{q_0}, k x^{2\kappa} w^{q_0 - 2})] . \end{aligned} \tag{3.17}$$

The error terms shown here arise from the higher-order excited states illustrated in (3.10) and (3.8); these will be considered further in Sec. III C.

TABLE I. Axial Boltzmann factors associated with adding a new spin to the left end of a chain of spins in the ANNNI model with $q_1=q_2=2$: each factor accounts for all broken nearest-neighbor and next-nearest-neighbor axial bonds emanating from the leftmost spin and extending to its right. The vertical bars denote the band edges separating adjacent ↑ and ↓ bands, and a circumflex identifies a spin which is flipped.

$s\,s\,\vert\,\hat{s}$	x^{κ}	$s\,\vert\,s\,\hat{s}$	x^{κ}	$s\,s\,\hat{s}$	$x^{-\kappa}$
$s\,\hat{s}\,\vert\,s$	x	$s\,\vert\,\hat{s}\,s$	x^{-1}	$s\,\hat{s}\,s$	x
$s\,\hat{s}\,\vert\,\hat{s}$	$x^{1+\kappa}$	$s\,\vert\,\hat{s}\,\hat{s}$	$x^{-1+\kappa}$	$s\,\hat{s}\,\hat{s}$	$x^{1-\kappa}$
$\hat{s}\,s\,\vert\,s$	$x^{1+\kappa}$	$\hat{s}\,\vert\,ss$	$x^{-1+\kappa}$	$\hat{s}\,s\,s$	$x^{1-\kappa}$
$\hat{s}\,s\,\vert\,\hat{s}$	x	$\hat{s}\,\vert\,s\,\hat{s}$	x^{-1}	$\hat{s}\,s\,\hat{s}$	x
$\hat{s}\,\hat{s}\,\vert\,s$	x^{κ}	$\hat{s}\,\vert\,\hat{s}\,s$	x^{κ}	$\hat{s}\,\hat{s}\,s$	$x^{-\kappa}$
$\hat{s}\,\hat{s}\,\vert\,\hat{s}$	1	$\hat{s}\,\vert\,\hat{s}\,\hat{s}$	1	$\hat{s}\,\hat{s}\,\hat{s}$	1

The next step (see I) would normally be to express $\overline{W}_2(l)$ as a sum of the $(k+1)$th powers of the two eigenvalues of $\mathbf{V}_0$. Notice, however, that $\mathbf{V}_0$ has a special triangular form and only a single eigenvalue λ_0: as mentioned above, one has $V_{12}\equiv 0$ because axial third-nearest-neighbor spins are not linked by any bond; moreover, $V_{11}=V_{22}$ because of the symmetry of the ANNNI model with respect to reflection in any lattice layer. The $(k+1)$th power of such a triangular matrix is simply

$$\mathbf{V}_0^{k+1}=\begin{bmatrix}\lambda_0^{k+1} & 0\\ -(k+1)\lambda_0^k x^{2\kappa-1}(1-x^2) & \lambda_0^{k+1}\end{bmatrix}, \tag{3.18}$$

whence one can directly compute the product in (3.17) to obtain (with $l=2k+3$)

$$\overline{W}_2(l)=(k+3)(1-x^2)(\lambda_0 w_0)^{k+2}\times[1+O(k^2x^{4\kappa}w^{q_0},kx^{2\kappa}w^{q_0-2})]\,. \tag{3.19}$$

This lowest-order result for the pair potential $\overline{W}_2(l)=(32^k3)$ agrees completely with that found by FS (Ref. 32) [see their Eq. (A2)]. For $k\geq 0$, $\overline{W}_2(l)$ is a positive, convex function, decaying exponentially and monotonically to 0 as $l\to\infty$. It therefore belongs to case A in the classification of two-wall interactions in I, and the naively predicted phase diagram would exhibit *all* simple periodic phases $\langle 2^k3\rangle$, $k\geq 1$, between $\langle 3\rangle$ and $\langle 2\rangle$ at any temperature $T\gtrsim 0$, as suggested by Fig. 2. One cannot, however, accept this indication of "devil's last step" or quasicontinuous behavior unreservedly without accounting for the $O(k^2w_0)$ corrections to (3.19), which clearly may become significant as $k\to\infty$ when T is *fixed*! In the context of the present transfer-matrix formulation, the danger can be identified in another way, namely, by considering the degeneracy of the matrix $\mathbf{V}_0$. The contributions of higher-order excited states of the lattice may well split its eigenvalues from the single value λ_0, leading to two distinct real or, perhaps, *complex* conjugate values, thereby *qualitatively* changing the form of $\overline{W}_2(l)$: recall that oscillatory potentials always belong to case B which entails a discontinuous rather than a quasicontinuous transition.

Before this problem is addressed, the results at leading order will be completed by calculating the three-wall potential $\overline{W}_3(l,l)=(32^k32^k3)$. Here the four layer sequences to be spanned by flipped spins are $2\nu'2$, $2\nu'3$, $3\nu'2$, and $3\nu'3$ with a core of $\nu'=2^k32^k$. As for (32^k3), each lowest-order chain of flipped spins spanning one of these layer sequences has exactly one flipped spin in each band. Because of the presence of the intermediate 3 band in the core ν', however, there is no longer as much freedom in the placement of these flipped spins: indeed, one can readily see that the middle layer of that 3 band must contain a flipped spin, and thereafter every second spin to right and left must be flipped. The presence of the 3 band within the core ν' is therefore properly described by the special transfer matrix

$$w_0\mathbf{C}=w_0\begin{bmatrix}0 & 0\\ (\underline{s\hat{s}s}\,\vert\,\hat{s}s)-(\underline{s\hat{s}s}\,\vert\,ss\cdots\underline{sss}\,\vert\,\hat{s}s) & 0\end{bmatrix}$$

$$=w_0\begin{bmatrix}0 & 0\\ x(1-x^{2\kappa}) & 0\end{bmatrix}, \tag{3.20}$$

whence, using (3.2),

$$\overline{W}_3(2k+3,2k+3)=(\mathbf{c}_0^{\dagger}-\mathbf{b}_0^{\dagger})\mathbf{V}_0^{k+1}\mathbf{C}\mathbf{V}_0^{k}(\mathbf{b}_1-\mathbf{c}_1)w_0^{2k+3}\times[1+O(k^2x^{4\kappa}w^{q_0},kx^{2\kappa}w^{q_0-2})]\,. \tag{3.21}$$

By employing (3.18) one can compute this product directly to obtain, finally (with $l=2k+3$),

$$\overline{W}_3(l,l)=-x^{2(1-\kappa)}\lambda_0(\lambda_0 w_0)^{2k+3}\times[1+O(k^2x^{4\kappa}w^{q_0},kx^{2\kappa}w^{q_0-2})]\,. \tag{3.22}$$

This result is also in agreement with the FS expression[32] [see their Eq. (A3)]. Since (neglecting again the correction factor) it suggests that $\overline{W}_3(l,l)<0$ for all $k\geq 0$, one would conclude from the discussion of Sec. V in I that every $\langle 2^k3\rangle$:$\langle 2^{k+1}3\rangle$ phase boundary of Fig. 2 is stable against any possible intermediate phases. With that, the refinement of the low-temperature phase diagram would be finished, all the results of FS having been completely recovered. If, however, one recognizes the danger posed by the factor $k^2w^{q_0}$, one sees that the FS conclusions are

justified provided that, on the kth boundary, the temperature remains less than

$$T_k^0 = q_0 J_0 / k_B \ln(c_0 k) ,$$

where $c_0 \gg 1$. [FS did not actually discuss the uniformity of their results in T and k but they left the impression that they would be uniform. It is worth stressing that the second correction term varying as kw^{q_0-2} is *unlikely* to be dangerous, since it may be, and, in fact, as seen below, is, simply generated by changes in the eigenvalues of $\mathbf{V}$ of order w^{q_0-2} which do not alter the *form* of $\overline{W}_2(l)$ or $\overline{W}_3(l,l)$.]

Using these explicit expressions for $\overline{W}_2$ and $\overline{W}_3$, which are valid at fixed $T \gtrsim 0$ at least for k not too large, one can isolate from $\overline{W}_3(l,l)$ the further-neighbor two-wall interaction $\overline{W}_2(2l)$ which is contained therein, according to the definition (2.26). Thus, the *residual three-wall potential* given by (see I, Sec. III)

$$\begin{aligned}\tilde{W}_3(l_1,l_2) &\equiv \overline{W}_3(l_1,l_2) - \overline{W}_2(l_1+l_2-1) \\ &= [(32^{k_1}32^{k_2}3) - (32^{k_1+k_2+1}3)] ,\end{aligned} \tag{3.23}$$

assumes, for $l_1 = l_2 \equiv l$, the value

$$\begin{aligned}\tilde{W}_3(l,l) &= -[2(k+2)(1-x^2) + x^{1-2\delta}(1-x^{2\kappa})] \\ &\quad \times [(1-x^{2\kappa})w_0]^{2k+3}[1+O(w_0)] \\ &\approx -2(k+2)[(1-x^{2\kappa})w_0]^{2k+3} .\end{aligned} \tag{3.24}$$

On the other hand, the three-wall potential as we have defined it is given by

$$\begin{aligned}\overline{W}_3(l,l) &= -x^{1-2\delta}(1-x^{2\kappa})[(1-x^{2\kappa})w_0]^{2k+3}[1+O(w_0)] \\ &\approx -x[(1-x^{2\kappa})w_0]^{2k+3} .\end{aligned} \tag{3.25}$$

In each of these expressions, the last form given is a valid approximation when $x \equiv e^{-2K_1} \ll 1$, as true in the low-temperature regime $w \equiv e^{-2K_0} \ll 1$ when $J_1 \simeq J_0$. One now sees that $\tilde{W}_3(l,l)$ is much *larger* in magnitude than $\overline{W}_3(l,l)$, being dominated by the contribution from $\overline{W}_2(l_1+l_2)$ in (3.23). This demonstrates the physical appropriateness of the definition of $\overline{W}_3$ introduced in I and adopted here.

C. Leading corrections to the two-wall potential

To go beyond these lowest-order results, one must sum the contributions of all the next-to-leading excited states of the lattice. As illustrated in (3.10) for (32^k3), such states are characterized by having an additional *in-chain* flipped spin, so that one band in the chain will have *two* spins flipped. This band will be neither in state 1 nor in state 2 as defined above, but in a new state, call it 3. It would therefore appear that the transfer matrix $\mathbf{V}_0$ must be enlarged to a 3×3 matrix to include this new state. In fact, however, because the chain may be disconnected *between* the two flipped spins of a band in state 3, such a "disconnected state 3" must be recognized as yet *another* distinct state of the band, call it 4. The reason for distinguishing between states 3 and 4 is that if a band m in, say, state 2 is added to the left of a band $m-1$ in state 3, the broken bonds between those two bands are different from what they would be if band $m-1$ were in state 4; in other words, $V_{23} \neq V_{24}$. Thus, $\mathbf{V}_0$ must be enlarged into a 4×4 matrix, $\mathbf{V}_1$, to allow for any band in the chain which may have both in-chain spins flipped. The upper left quadrant of $\mathbf{V}_1$ is just $\mathbf{V}_0$ again; the additional entries of $\mathbf{V}_1$, involving bands in states 3 and 4, are listed explicitly in Table II, along with the definitions of states 1–4. Note that all entries of the form V_{4j} must carry an extra factor of -1 to satisfy Rule 2. When these V_{ij} are evaluated using the Boltzmann factors of Table I, one obtains

$$\mathbf{V}_1 = \begin{bmatrix} \lambda_0 & 0 & x^\kappa\lambda_0 & x^\kappa V_{11} \\ -x^{2\kappa-1}(1-x^2) & \lambda_0 & -x^{\kappa-1}(x^{2\kappa}-x^2) & x^\kappa V_{21} \\ -x^{\kappa-2}(x^{2\kappa}-x^2)w_0 & x^{\kappa-1}\lambda_0 w_0 & (1-x^{4\kappa-2})w_0 & x^\kappa V_{31} \\ -x^{\kappa+1}V_{21}w_0 & -x^{\kappa+1}V_{22}w_0 & -x^{\kappa+1}V_{23}w_0 & x^\kappa V_{41} \end{bmatrix} . \tag{3.26}$$

Notice that all entries V_{3j} and V_{4j} of $\mathbf{V}_1$ carry an additional factor w_0 because of the extra flipped spin in the band. The identities

$$V_{i4} = x^\kappa V_{i1}, \quad \text{for all } i \tag{3.27}$$

$$V_{4j} = -x^{\kappa+1}V_{2j}w_0, \quad \text{for all } j \tag{3.28}$$

arise directly from the separated nature of the band in state 4, as is evident from the expressions of Table II.

Now, adopting $\mathbf{V}_1$ as the transfer matrix in the form analogous to (3.17) adds to the lowest-order result for $\overline{W}_2(l)$ not only the leading correction, which determines the nature of the splitting of the two eigenvalues λ_0, but also higher-order corrections, arising from the presence of more than one additional in-chain flipped spin. These latter corrections, which can be identified by the additional factors of w_0 that they carry, are not of prime interest here. Moreover, they are, in any case, less significant than the higher-order correction due to flipping an extra spin *outside* the chain [as illustrated in (3.8)], which has so far been ignored but will be considered later. Indeed, the full 4×4 matrix formalism is not actually needed to ascertain the effects of the *leading* corrections: as shown below in Sec. III E, an appropriately modified 2×2 matrix formalism suffices.

To adapt the form (3.17) to the 4×4 matrix $\mathbf{V}_1$, one needs the appropriate four-component versions of the vectors $\mathbf{b}_i$ and $\mathbf{c}_i$ $(i=0,1)$. To leading order, these are

$$\mathbf{b}_0^\dagger=[\underline{ss}\,|\,\hat{s}s\,|\,,\underline{ss}\,|\,s\hat{s}\,|\,,\underline{ss}\,|\,\hat{s}\hat{s}\,|\,,(\underline{ss}\,|\,\hat{s}s\,|\,\cdots\underline{ss}\,|\,s\hat{s})]$$
$$=[x^{\kappa-1},x^{\kappa},x^{2\kappa-1},x^{2\kappa-1}]\,, \tag{3.29}$$

$$\mathbf{c}_0^\dagger=[\underline{s}\,|\,s\hat{s}s\,|\,,\underline{s}\,|\,ss\hat{s}\,|\,,\underline{s}\,|\,s\hat{s}\hat{s}\,|\,,(\underline{s}\,|\,s\hat{s}s\,|\,\cdots\underline{s}\,|\,ss\hat{s})]$$
$$=[x^{\kappa+1},x^{-\kappa},x,x]\,,$$

where we have not troubled to distinguish them from the two-component forms, and

$$\mathbf{b}_1=\begin{bmatrix}|\,\hat{s}s\,|\,ss\\ |\,s\hat{s}\,|\,ss\\ |\,\hat{s}\hat{s}\,|\,ss\\ |\,\hat{s}s\,|\,ss\cdots s\hat{s}\,|\,ss\end{bmatrix}=\begin{bmatrix}x^{\kappa+1}\\ x^{\kappa}\\ x^{2\kappa-1}w_0\\ -x^{2\kappa+1}w_0\end{bmatrix},$$
$$\mathbf{c}_1=\begin{bmatrix}|\,\hat{s}ss\,|\,s\\ |\,s\hat{s}s\,|\,s\\ |\,\hat{s}\hat{s}s\,|\,s\\ |\,\hat{s}ss\,|\,s\cdots|\,s\hat{s}s\,|\,s\end{bmatrix}=\begin{bmatrix}x^{1-\kappa}\\ x^{\kappa+2}\\ xw_0\\ -x^3w_0\end{bmatrix}. \tag{3.30}$$

Since the rank of $\mathbf{V}_1$ is only three, one of its eigenvalues is identically zero; the other three satisfy the cubic equation

$$\lambda^3+\alpha_2\lambda^2+\alpha_1\lambda+\alpha_0=0\,, \tag{3.31}$$

with

$$\alpha_2\equiv-2\lambda_0-w_0[1-x^{4\kappa}-x^{4\kappa-2}(1-x^2)^2]\,,$$
$$\alpha_1\equiv\lambda_0^2(1+2w_0+w_0^2x^{4\kappa}),\quad \alpha_0\equiv-\lambda_0^4w_0\,. \tag{3.32}$$

According to the standard method of solving a cubic equation,[38] one defines

$$Q\equiv\tfrac{1}{3}\alpha_1-\tfrac{1}{9}\alpha_2^2$$
$$=-[\tfrac{1}{3}\lambda_0(1+w_0)]^2\{1-\lambda_0w_0[4\mu(x)+O(w_0)]\}\,, \tag{3.33}$$

$$R\equiv\tfrac{1}{6}\alpha_1\alpha_2-\tfrac{1}{2}\alpha_0-\tfrac{1}{27}\alpha_2^3$$
$$=-[\tfrac{1}{3}\lambda_0(1+w_0)]^3(1+\lambda_0w_0\{\tfrac{3}{2}[5\mu(x)-9]+O(w_0)\})\,, \tag{3.34}$$

where for brevity we have introduced

$$\mu(x)\equiv1+x^{4\delta}(1-x^2)^2/\lambda_0^2\,, \tag{3.35}$$

with, as before, $\delta=\kappa-\frac{1}{2}$. Now there will be a complex conjugate pair of roots if and only if[38]

$$D\equiv Q^3+R^2>0\,. \tag{3.36}$$

In the present case it is easy to check this condition since one has

$$D=\tfrac{1}{27}x^{4\delta}(1-x^2)^2\lambda_0^5w_0[1+O(w_0)]>0\,. \tag{3.37}$$

This result is valid for *all* x in (0,1): D vanishes at least as fast as $(1-x)^7$ when $x\to1-$, and at least as fast as $x^{4\delta}$ when $x\to0+$. (We will only need $\delta>0$.) This observation will be useful when examining the results in the highly anisotropic regime (3.3), in which $x\to1$ and the Villain-Gordon harmonic approximation to mean-field theory[29] is valid.

Provided the magnitude of these two complex roots dominates that of the remaining real root (as verified below), one can immediately conclude that the two-wall potential $\overline{W}_2(l)$ is an exponentially damped sinusoidal function, exhibiting a negative absolute minimum and hence belonging to case B. Consequently, as explained, there can be *no* devil's last step in the phase diagram at any fixed temperature $T\gtrsim0$.

To make these observations more quantitative, set

$$S_\pm\equiv(R\pm\sqrt{D}\,)^{1/3}$$
$$=-\tfrac{1}{3}\lambda_0(1+w_0)+\tfrac{1}{6}\lambda_0^2w_0[3+\mu(x)+O(w_0)]$$
$$\pm x^{2\delta}(1-x^2)(\tfrac{1}{3}\lambda_0w_0)^{1/2}[1+O(w_0)]\,. \tag{3.38}$$

Then the two complex eigenvalues are found to be[38]

$$\lambda_\pm=\lambda_0[1+O(w_0)]\pm ix^{2\delta}(1-x^2)(\lambda_0w_0)^{1/2}[1+O(w_0)]\,, \tag{3.39}$$

while the remaining real eigenvalue is

$$\lambda_3=(S_++S_-)-\tfrac{1}{3}\alpha_2=\lambda_0^2w_0[1+O(w_0)]\,. \tag{3.40}$$

Since the magnitude of λ_3 is smaller than that of $\lambda_\pm$ by a factor λ_0w_0, one obtains, from the analog of (3.17), the simple form

$$\overline{W}_2(l)=2w_0^{k+2}\,\mathrm{Re}\{A_+\lambda_+^{k+1}\}[1+O(w_0)]\,, \tag{3.41}$$

where

$$A_+\equiv|\,A\,|\,e^{i\phi} \tag{3.42}$$

is a complex amplitude to be determined, while the correction term subsumes the additional term in λ_3^{k+1}. Note that the leading forms (3.39) and (3.40) for the eigenvalues $\lambda_\pm$ and λ_3 could, of course, be obtained by perturbation theory from the characteristic equation (3.31), without resorting to the general cubic solution.

At this point one can also consider the effect of the further corrections arising from extra spins which are flipped *outside* the chain, the principal contribution being that illustrated in (3.8). One may incorporate these extra excited states into the present transfer-matrix formalism by replacing each matrix element V_{ij} by a matrix $\mathbf{V}_{ij}$. The apparent correction to $\overline{W}_2(l)$ of $O(kx^{2\kappa}w^{q_0-2})$ associated with (3.8) is then seen to reflect a shift in the leading eigenvalues $\lambda_\pm$ (as mentioned above): the result (3.39) becomes

$$\lambda_\pm=\lambda_0[1\pm ic_2(x)(w_0)^{1/2}+O(x^{2\kappa}w^{q_0-2})]\,, \tag{3.43}$$

where the abbreviation

$$c_2(x)\equiv x^{2\delta}(1-x^2)\lambda_0^{-1/2}\sim(1-x)^{1/2}\,, \tag{3.44}$$

as $x\to1$, has been introduced. Note that, as written, (3.43) also implies that each additive correction term to the $\lambda_\pm$ vanishes like $\lambda_0(x)$, i.e., at least as fast as $(1-x)$, when $x\to1$. This feature is to be expected on quite gen-

TABLE II. Definitions of the four possible states of a band when arbitrarily many in-chain spin flips are allowed, and expressions for the entries of the transfer matrix $\mathbf{V}_1$ involving states 3 and 4. Bands being added to the chain in each case are underlined.

Band state:	1	2	3	4
Layers with spins flipped:	$\lvert\hat{s}\,\underline{s}\rvert$ (first)	$\lvert s\,\underline{\hat{s}}\rvert$ (second)	$\lvert\hat{s}\,\underline{\hat{s}}\rvert$ (both)	$\lvert\hat{s}\,\underline{s}\rvert\cdots\lvert s\,\underline{\hat{s}}\rvert$ (both and separated)

$V_{13}=(\underline{\hat{s}}\mid\hat{s}\,\hat{s})-(\underline{\hat{s}}\mid ss\cdots\underline{ss}\mid\hat{s}\,\hat{s})$,

$V_{14}=(\underline{\hat{s}}\mid\hat{s}s\cdots\underline{ss}\mid s\hat{s})-(\underline{\hat{s}}\mid ss\cdots\underline{ss}\mid\hat{s}s\cdots\underline{ss}\mid s\hat{s})$

$V_{23}=(\underline{s\hat{s}}\mid\hat{s}\,\hat{s})-(\underline{s\hat{s}}\mid ss\cdots\underline{ss}\mid\hat{s}\,\hat{s})$,

$V_{24}=(\underline{s\hat{s}}\mid\hat{s}s\cdots\underline{ss}\mid s\hat{s})-(\underline{s\hat{s}}\mid ss\cdots\underline{ss}\mid\hat{s}s\cdots\underline{ss}\mid s\hat{s})$

$V_{31}=(\underline{\hat{s}\,\hat{s}}\mid\hat{s}s)-(\underline{\hat{s}\,\hat{s}}\mid ss\cdots\underline{ss}\mid\hat{s}s)$,

$V_{32}=(\underline{\hat{s}\,\hat{s}}\mid s\hat{s})-(\underline{\hat{s}\,\hat{s}}\mid ss\cdots\underline{ss}\mid s\hat{s})$

$V_{33}=(\underline{\hat{s}\,\hat{s}}\mid\hat{s}\,\hat{s})-(\underline{\hat{s}\,\hat{s}}\mid ss\cdots\underline{ss}\mid\hat{s}\,\hat{s})$,

$V_{34}=(\underline{\hat{s}\,\hat{s}}\mid\hat{s}s\cdots\underline{ss}\mid s\hat{s})-(\underline{\hat{s}\,\hat{s}}\mid ss\cdots\underline{ss}\mid\hat{s}s\cdots\underline{ss}\mid s\hat{s})$

$V_{41}=-(\underline{\hat{s}s}\mid ss\cdots\underline{s\hat{s}}\mid\hat{s}s)+(\underline{\hat{s}s}\mid ss\cdots\underline{s\hat{s}}\mid ss\cdots\underline{ss}\mid\hat{s}s)$

$V_{42}=-(\underline{\hat{s}s}\mid ss\cdots\underline{s\hat{s}}\mid s\hat{s})+(\underline{\hat{s}s}\mid ss\cdots\underline{s\hat{s}}\mid ss\cdots\underline{ss}\mid s\hat{s})$

$V_{43}=-(\underline{\hat{s}s}\mid ss\cdots\underline{s\hat{s}}\mid\hat{s}\,\hat{s})+(\underline{\hat{s}s}\mid ss\cdots\underline{s\hat{s}}\mid ss\cdots\underline{ss}\mid\hat{s}\,\hat{s})$

$V_{44}=-(\underline{\hat{s}s}\mid ss\cdots\underline{s\hat{s}}\mid\hat{s}s\cdots\underline{ss}\mid s\hat{s})+(\underline{\hat{s}s}\mid ss\cdots\underline{s\hat{s}}\mid ss\cdots\underline{ss}\mid\hat{s}s\cdots\underline{ss}\mid s\hat{s})$

eral grounds. First observe that each entry V_{ij} of the matrix $\mathbf{V}_1$ in (3.26) vanishes like $(1-x)$. This is due to the separation of the chain which can occur between any two flipped spins: the connected and disconnected configurations contributing to V_{ij} exhibit identical powers of w but different powers of x; since the disconnected configuration carries an extra minus sign, their sum V_{ij} must therefore vanish as $x\to 1$. (See the expressions of Table II.) Now even if arbitrarily many spins are flipped in each layer of the chain, this argument still applies to show that each element of each matrix $\mathbf{V}_{ij}$, and hence every eigenvalue of $\mathbf{V}$, must again vanish like $(1-x)$. Consequently, one sees from the general analog of (3.17) that $\overline{W}_2(l)$ must vanish like $(1-x)^{k+3}$, the additional two factors of $(1-x)$ coming from the vector differences $(\mathbf{c}_0^\dagger-\mathbf{b}_0^\dagger)$ and $(\mathbf{b}_1-\mathbf{c}_1)$ [see (3.29) and (3.30)].

The error terms in (3.43) are negligible provided $x^2 w^{q_0-4}\ll 1-x$, or

$$(q_0-4)J_0+2J_1\gg k_B T\ln(1-x)^{-1}\ . \tag{3.45}$$

This constraint covers the ANNNI model with isotropic couplings on a simple cubic lattice ($J_0=J_1$, $q_0=4$), favored for numerical studies.

To evaluate the amplitude A_+ in (3.41) and complete the calculation of $\overline{W}_2(l)$, it is not actually necessary to obtain the eigenvectors of $\mathbf{V}_1$. Instead, using (3.43) for λ_+, one can expand (3.41) as a formal power series in k, and equate the coefficients of k^0 and k with the corresponding coefficients in the expression (3.19) for $\overline{W}_2(l)$. Equivalently, one could equate (3.19) and (3.41) directly for $k=0,1$. In either case, solving the resulting equations yields

$$\begin{aligned}\lvert A\rvert&=\frac{\lambda_0(1-x^2)}{2c_2(x)(w_0)^{1/2}}[1+x\mathcal{E}(x,w)]\ ,\\ \phi&=-\tfrac{1}{2}\pi+2c_2(x)(w_0)^{1/2}[1+x\mathcal{E}(x,w)]\ ,\end{aligned} \tag{3.46}$$

where the magnitude of error is indicated conveniently by the new *order symbol*

$$\mathcal{E}(x,w)\equiv O\{[w^{q_0-4}/(1-x)]^{1/2}\}\ . \tag{3.47}$$

Thus, with (3.14) and (3.44), the pair potential is finally given by

$$\begin{aligned}\overline{W}_2(l)=\lambda_0 x^{-2\delta}&\{\lambda_0 w_0[1+x\mathcal{E}(x,w)]\}^{k+3/2}\\ &\times\sin\{(k+3)c_2(x)(w_0)^{1/2}[1+x\mathcal{E}(x,w)]\}\ .\end{aligned} \tag{3.48}$$

For $l\equiv 2k+3$ sufficiently small that the sine can be linearized, one recovers the FS result (3.19), as must happen. For larger l, however, $W_2(l)$ becomes negative, as sketched in Fig. 3, having an absolute minimum at $l_{\max}=2k_{\max}+3$ with

$$k_{\max}(T)=[\pi/c_2(x)(w_0)^{1/2}][1+x\mathcal{E}(x,w)]\ . \tag{3.49}$$

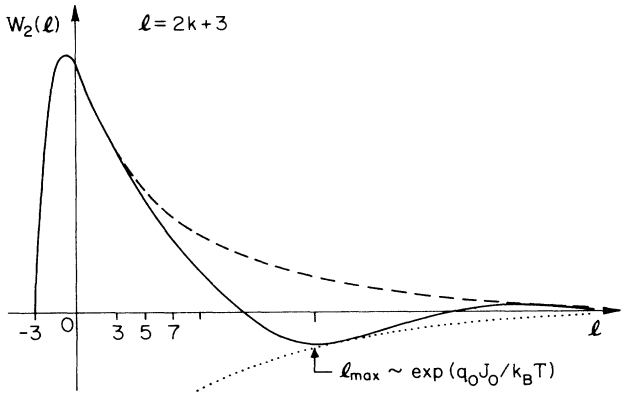

FIG. 3. Character of the wall pair interaction $W_2(l)$ with $l=2k+3$ for the ANNNI model, for axial coordination numbers $q_1=q_2=2$. The solid curve represents the complete expression (3.48), while the dashed curve shows the "short-distance" approximation obtained by linearizing the sine function. The dotted curve depicts the overall exponential envelope. The minimum at $k_{\max}$ moves to ∞ as $T\to 0$.

Note also that $W_2(l)$ is a convex function on $[1, l_{\max}]$: by using the "short-distance" expression $W_2(l) \propto (k+3)(\lambda_0 w_0)^{k+2}$, one can easily check that when $\ln w_0 < -1$ (or $k_B T < 2q_0 J_0$) the maximum of $\overline{W}_2(l)$ is at $l < -1$ and its point of inflection is at $l < 1$, as indicated in Fig. 3. One therefore concludes that, among the simple periodic phases $\langle 2^k 3 \rangle$, only those with $1 \le k < k_{\max}$ appear between $\langle 3 \rangle$ and $\langle 2 \rangle$ at any fixed small temperature. Since the cutoff spacing, $k_{\max}$, *diverges* as $T \to 0$, however, it is still true that *all* phases of the form $\langle 2^k 3 \rangle$ spring from the multiphase point ($\kappa = \frac{1}{2}$, $T = 0$), as illustrated in Fig. 2. Recall from I that the phase widths decrease exponentially fast as k increases, according to

$$\Delta\kappa_k(T) \sim K_1^{-1} k^2 w_0^{k+1} \quad \text{for } \langle 2^k 3 \rangle \, . \tag{3.50}$$

Another, surprising, aspect of the result (3.48) is seen when one compares $\overline{W}_2(l)$ to the corresponding two-wall interaction $\beta U_1(2k+3)$ in the notation of the Villain-Gordon approximation to mean-field theory.[29] In the regime (3.3), which can be seen to limit the validity of their treatment, one has

$$\begin{aligned} x &= e^{-2K_1} \approx 1 - 2K_1, \quad \lambda_0 = 1 - x^{2\kappa} \approx 4 \mid K_2 \mid \, , \\ c_2(x) &= x^{2\delta}(1-x^2)\lambda_0^{-1/2} \approx \kappa^{-1}(4 \mid K_2 \mid)^{1/2} \, , \end{aligned} \tag{3.51}$$

so that the result (3.48) reduces to

$$\begin{aligned} \overline{W}_2(l) \approx{}& 4 \mid K_2 \mid (4 \mid K_2 \mid w_0)^{k+3/2} \\ & \times \sin[\kappa^{-1}(k+3)(4 \mid K_2 \mid w_0)^{1/2}] \, . \end{aligned} \tag{3.52}$$

This agrees completely with the expression for $\beta U_1(2k+3)$: see Eq. (7.25) of Villain and Gordon.[29] Such full agreement is surprising because the calculations of this section assume axial coordination numbers $q_1 = q_2 = 2$, whereas mean-field theory should correspond to the limit $q_i \to \infty$ with $q_i J_i$ fixed. One is thus led to guess that the results found here for the ANNNI model remain *qualitatively unchanged* under variation of q_i. It should, however, be recalled that the Villain-Gordon results are (so far) known to be valid only for the "intermediate" temperature regime (3.3): at lower temperatures, or for isotropic couplings, one might well anticipate qualitative differences between the original ($q_1 = q_2 = 2$) ANNNI model and its mean-field limit. In Sec. III F, however, the present transfer-matrix calculations are generalized to arbitrary q_i, and it is seen explicitly that *no* such differences do, in fact, arise!

D. Three-wall potential in second order

The three-wall interaction $\overline{W}_3(l,l)$, governed by the eigenvalues $\lambda_\pm$ of $\mathbf{V}_1$ according to the 4×4 analog of (3.21), must assume the general form

$$\begin{aligned} \overline{W}_3(l,l) = 2w_0^{2k+3} \, \mathrm{Re}\{ & A_{++}\lambda_+^{2k+1} \\ & + A_{+-}\lambda_+^{k+1}\lambda_-^{k} \}[1 + O(w_0)] \, , \end{aligned} \tag{3.53}$$

where, for $k \ge 1$, the error term subsumes the terms of order $\lambda_0^{k+1}\lambda_3^k$ which arise from smaller eigenvalues. [As in (3.41) for $\overline{W}_2(l)$, taking the real part in (3.53) accounts for the complex conjugate terms $A_{--}\lambda_-^{2k+1}$ and $A_{-+}\lambda_-^{k+1}\lambda_+^k$.] Using (3.43) for $\lambda_\pm$ and adopting the error notation of (3.47), one can rewrite this as

$$\overline{W}_3(l,l) = 2w_0^{2k+3}\{\lambda_0[1 + O(x^{2\kappa} w^{q_0 - 2})]\}^{2k+1}(A \cos\{2(k+1)c_2(x)(w_0)^{1/2}[1 + x\mathcal{E}(x,w)] + \phi\} + B) \, , \tag{3.54}$$

where the real amplitudes $A > 0$ and B, and the phase angle ϕ, are again to be determined. Once more, it is simpler to bypass the computation involving eigenvectors of $\mathbf{V}_1$ by expanding as a power series in k and equating the coefficients with those in (3.22), which one may write as

$$\overline{W}_3(l,l) = \lambda_0^{2k+4} w_0^{2k+3}[-x^{2(1-\kappa)} + k^2 d(x) w_0 + O(x^{2\kappa} w^{q_0 - 2}, k x^{2\kappa} w^{q_0 - 2}, k^2 x^{4\kappa} w^{2q_0 - 4})] \, . \tag{3.55}$$

Here the leading term in k^2, arising from an extra in-chain spin flip as explained in association with (3.10), has been explicitly displayed: the unknown amplitude $d(x)$ will be needed. Equating coefficients of k^p for $p = 0, 1, 2$ leads to

$$\begin{aligned} B &= -\tfrac{1}{2}\lambda_0^3 x^{2(1-\kappa)}[1 + O(w^{q_0 - 2})] - A\cos\phi \, , \\ \phi &= \pi + x\mathcal{E}(x,w) \, , \\ A &= \frac{\lambda_0^3}{4c_2^2(x)}[d(x) + O(x^{4\kappa} w^{q_0 - 4})][1 + x\mathcal{E}(x,w)] \, . \end{aligned} \tag{3.56}$$

It remains to find $d(x)$. This is readily done, since only the coefficient of k^2 associated with flipping an extra spin in the chain is required. As in (3.10), the presence of this extra flipped spin permits the formation of two unbound defects as shown in Table III. These defects may be in any of the 2 bands of the chain, provided they do not interact with each other, with the interior 3 band, or with the ends of the chain, since such "edge effects" would contribute at order k or order k^0 but not at order k^2. The two defects may be either on opposite sides of the interior 3 band, as shown in (a) of Table III, or on the same side, as in (b) and (c). Clearly the contributions of (b) and (c) will be equal. Allowing for a possible separation of the chain between any two flipped spins according to Rule 2, one can refer to Table I (or use the matrix elements of $\mathbf{V}_1$ for the 2 bands) to compute the Boltzmann factor of each chain, as also recorded in Table III: note that the endmost flipped spins may lie within either 2 or 3 bands. Summing over those possibilities with signs as given by Rule 1, one finds

$$d(x) = (1 - x^2)^2(1 + 2x^{2\kappa})/\lambda_0 \, . \tag{3.57}$$

On substituting this result into (3.56) and thence into (3.54), one concludes

TABLE III. Chains of flipped spins contributing at next-to-leading order to the three-wall interaction $\overline{W}_3(l,l)$ of the ANNNI model, when $q_1=q_2=2$. The Boltzmann factor of each chain (including decompositions) is also given: those for (b) and (c) are equal.

(a) $\left|\begin{matrix} |\,s\hat{s} \\ |\,ss\hat{s} \end{matrix}\right| \underbrace{s\hat{s}\,|\,s\hat{s}\,|\,s\hat{s}\,|\,\hat{s}s\,|\,\hat{s}s\,|}_{k\text{ 2-bands}} \quad \underbrace{\hat{s}s\hat{s}\,|\,s\hat{s}\,|\,\hat{s}s\,|\,\hat{s}s\,|\,\hat{s}s\,|\,\hat{s}s}_{k\text{ 2-bands}} \left|\begin{matrix} \hat{s}s\,|\,s \\ \hat{s}ss\,| \end{matrix}\right.$

$$= \begin{matrix} x^{\kappa} \\ x^{-\kappa} \end{matrix} \Big\} [-x^{2\kappa}(1-x^2)^2\lambda_0^{2k+1}w_0^{2k+3}] \Big\{ \begin{matrix} x^{\kappa} \\ x^{-\kappa} \end{matrix}$$

(b) $\left|\begin{matrix} |\,s\hat{s} \\ |\,ss\hat{s} \end{matrix}\right| s\hat{s}\,|\,\hat{s}s\,|\,\hat{s}s\,|\,\hat{s}\hat{s}\,|\,s\hat{s}\,|\,s\hat{s}s\,|\,\hat{s}s\,|\,\hat{s}s\,|\,\hat{s}s\,|\,\hat{s}s\,|\,\hat{s}s\,| \left|\begin{matrix} \hat{s}s\,|\,s \\ \hat{s}ss\,| \end{matrix}\right.$

$$= \begin{matrix} x^{\kappa} \\ x^{-\kappa} \end{matrix} \Big\} [-x^{4\kappa}(1-x^2)^2\lambda_0^{2k+1}w_0^{2k+3}] \Big\{ \begin{matrix} x^{\kappa} \\ x^{-\kappa} \end{matrix}$$

(c) $\left|\begin{matrix} |\,s\hat{s} \\ |\,ss\hat{s} \end{matrix}\right| s\hat{s}\,|\,s\hat{s}\,|\,s\hat{s}\,|\,s\hat{s}\,|\,s\hat{s}\,|\,s\hat{s}s\,|\,\hat{s}s\,|\,\hat{s}s\,|\,\hat{s}\hat{s}\,|\,s\hat{s}\,|\,\hat{s}s \left|\begin{matrix} \hat{s}s\,|\,s \\ \hat{s}ss\,| \end{matrix}\right.$

$$\overline{W}_3(l,l)=\frac{w_0^{2k+3}}{2x^{4\delta}}\{\lambda_0[1+O(x^{2\kappa}w^{q_0-2})]\}^{2k+4}\{1+x\,\mathcal{E}(x,w)-(1+2x^{2\kappa})\cos[2(k+1)c_2(x)(w_0)^{1/2}+x\,\mathcal{E}(x,w)]\}\ . \tag{3.58}$$

This form has rather interesting consequences. Observe first that when k is small enough the cosine may be replaced by unity, and the lowest-order FS result (3.22) is then recovered: since $\overline{W}_3(l,l)$ is negative, the $\langle 2^k3\rangle$:$\langle 2^{k+1}3\rangle$ boundary is stable against the appearance of intermediate phases. However, since the amplitude of the cosine in (3.58) *exceeds* the remaining constant within the braces, $\overline{W}_3(l,l)$ must eventually *change sign* as l increases. Moreover, since the argument of the cosine is essentially *twice* that of the sine appearing in $\overline{W}_2(l)$ in (3.48), $\overline{W}_3(l,l)$ will change sign *before* l has increased to its maximum value $l=l_{\max}-1=2k_{\max}+2$ given by (3.49). More precisely, $\overline{W}_3(l,l)$ vanishes at $l^{(1)}=2k^{(1)}+3$ where

$$k^{(1)}(T)=[x^{\kappa}/c_2(x)(w_0)^{1/2}][1+O(x)+\mathcal{E}(x,w)]$$
$$\approx(x^{\kappa}/\pi)k_{\max}\ . \tag{3.59}$$

For larger l, $\overline{W}_3(l,l)$ remains positive until it changes sign a second time at $l^{(2)}=2k^{(2)}+3$ with

$$k^{(2)}(T)=[1/c_2(x)(w_0)^{1/2}]\{\pi-x^{\kappa}[1+O(x)+\mathcal{E}(x,w)]\}$$
$$\approx k_{\max}-k^{(1)}\ , \tag{3.60}$$

after which $\overline{W}_3(l,l)$ remains negative while l increases to $l_{\max}-1$. Consequently, as illustrated in Fig. 4, the *mixed phases* $\langle 2^k32^{k+1}3\rangle$ appear for $k^{(1)}(T)<k<k^{(2)}(T)$. Note that although $k^{(1)}\to\infty$ as $T\to0$, one also has $k^{(1)}/k_{\max}\to0$ in the same limit, and hence $k^{(2)}/k_{\max}\to1$. Thus there are $\langle 2^k32^{k+1}3\rangle$ phases appearing arbitrarily close to the zero-temperature multiphase point at $\kappa=\frac{1}{2}$. These refinements of the FS diagram are quite surprising but their dependence on $\overline{W}_3$ makes their nature understandable!

It is also instructive to compare the exact result (3.58) for $\overline{W}_3(l,l)$ to the corresponding expression which follows from the approximate mean-field approach of Villain and Gordon.[29] Their effective Hamiltonian for the ANNNI model contains only *pairwise* interactions between domain walls (although the potential between two walls depends on the number of intermediate walls and hence is not a true pair potential). For such a model, as discussed in Sec. III of I, the three-wall potential $\overline{W}_3(l,l)$ is simply given by the further-neighbor pair interaction $\beta U_2(4k+6)$. This quantity is readily evaluated from Eq. (7.22b) of Villain and Gordon,[29,17] as

$$\overline{W}_3(l,l)\cong\beta U_2(4k+6)=-4\,|\,K_2\,|\,(4\,|\,K_2\,|\,w_0)^{2k+3}[1+O(\beta w_0)]\cos\{\kappa^{-1}(2k+\tfrac{9}{2})(4\,|\,K_2\,|\,w_0)^{1/2}[1+O(\beta w_0)]\}\ . \tag{3.61}$$

By contrast, in the regime (3.3) where the Villain-Gordon approximation is valid, our exact result (3.58) simplifies to

$$\overline{W}_3(l,l)=2\,|\,K_2\,|\,\{4\,|\,K_2\,|\,w_0[1+O(w^{q_0-2})]\}^{2k+3}$$
$$\times\{1+\mathcal{E}(x,w)-[3+O(K_1)]\cos[2\kappa^{-1}(k+1)(4\,|\,K_2\,|\,w_0)^{1/2}+\mathcal{E}(x,w)]\}\ . \tag{3.62}$$

Both these expressions for $\overline{W}_3(l,l)$ are negative for small k, change sign at some $k=k^{(1)}(T)$, and then remain positive over the interval $(k^{(1)},k_{\max}-k^{(1)})$; but for the Villain-Gordon result (3.61), one has

$$k^{(1)}(T)\approx\tfrac{1}{4}\pi\kappa(4\,|\,K_2\,|\,w_0)^{-1/2}\ , \tag{3.63}$$

whereas the exact result (3.62) yields

$$k^{(1)}(T)\approx\tfrac{1}{2}(\cos^{-1}\tfrac{1}{3})\kappa(4\,|\,K_2\,|\,w_0)^{-1/2}\ . \tag{3.64}$$

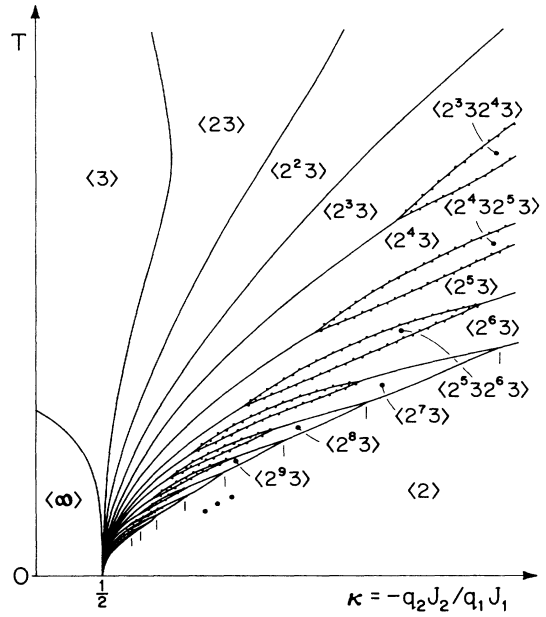

FIG. 4. Schematic phase diagram of the ANNNI model in the plane of competition ratio κ vs temperature T, as deduced under the low-temperature condition $w_0=\exp(-2q_0J_0/k_BT)\ll 1$. Solid lines represent stable, first-order transitions (although under sufficiently anisotropic conditions the phase $\langle 4\rangle$ and, possibly, others, will appear on the $\langle\infty\rangle$:$\langle 3\rangle$ boundary—see text). At fixed $T>0$, simple periodic phases $\langle 2^k3\rangle$ appear between $\langle 3\rangle$ and $\langle 2\rangle$ only for $1\le k<k_{\max}$, where $k_{\max}\sim w_0^{-1/2}\to\infty$ as $T\to 0$: this gives rise to a series of $\langle 2^k3\rangle$:$\langle 2^{k+1}3\rangle$:$\langle 2\rangle$ triple points marked by vertical ticks along the $\langle 2\rangle$ phase boundary. Mixed phases, $\langle 2^k32^{k+1}3\rangle$, are also present, for $k^{(1)}<k<k^{(2)}$, where $k^{(1)}\approx(x^\kappa/\pi)k_{\max}$ and $k^{(2)}\approx k_{\max}-k^{(1)}$. The boundaries of these mixed phases have been decorated with dots since they may be unstable to the appearance of higher-order mixed phases. The phase widths, which decrease exponentially fast as k increases, have been greatly exaggerated here for clarity. The phase diagram remains qualitatively unchanged under variation of q_1 and q_2 from 2 to ∞ (the mean-field limit).

Since $\frac{1}{4}\pi\simeq 0.785$ while $\frac{1}{2}(\cos^{-1}\frac{1}{3})\simeq 0.616$, one sees that the Villain-Gordon approximation remains *qualitatively correct* in implying the existence of an interval of values $[k^{(1)}(T),\ k_{\max}(T)-k^{(1)}]$ over which the intermediate phases $\langle 2^k32^{k+1}3\rangle$ appear, but the quantitative estimate of $k^{(1)}$ is too large by some 28% (thus *under*estimating the width of the interval). In fact, however, Villain and Gordon did not describe any of the mixed phases that arise from their formalism.

The stability of the $\langle 2^k3\rangle$:$\langle 2^k32^{k+1}3\rangle$ and $\langle 2^k32^{k+1}3\rangle$:$\langle 2^{k+1}3\rangle$ boundaries (marked by dots in Fig. 4), which is governed by $\overline{W}_4$, has not been checked here. It is clear, however, by analogy with (3.53), that $\overline{W}_n(l_1,l_2,\ldots,l_{n-1})$ will contain a term with the factor

$$\cos[(l_1+l_2+\cdots+l_{n-1})c_2(x)(w_0)^{1/2}+\phi_n]\ ,$$

which oscillates increasingly fast as n increases. This situation could well lead to a complex variety of higher-order mixed phases, arbitrarily close to the multiphase point. The Villain-Gordon approximation may or may not provide a qualitatively correct reproduction of such further structure, but we suspect, on the basis of the explicit results for $\overline{W}_2$ and $\overline{W}_3$ examined so far, that their approximation would become increasingly poor for such higher-order phases.

At this point we may remark that since the $\langle 3\rangle$:$\langle 23\rangle$ boundary is known to be stable at low T against $\langle 23^k\rangle$ and all other mixed phases, there is nothing to be gained by reversing point of view and regarding the 2 *bands* as walls separating $\langle 3\rangle$-*phase* domains. The $\langle 3\rangle$:$\langle 23\rangle$ boundary may become unstable only where the validity of the present analysis breaks down, i.e., at temperatures at or above $k_BT\sim J_0$: there the numerical mean-field results of Selke and Duxbury[24,25] indicate that such destabilization *does* in fact occur.

To complete this discussion of the low-temperature phase diagram of the ANNNI model, it is appropriate to reconsider the $\langle\infty\rangle$:$\langle 3\rangle$ boundary. In Sec. II A we noted that the first step of the FS free energy expansion determines this boundary as marking a stable, first-order transition, *except* in the anisotropic cases $x<w_0$ (i.e., $J_1>q_0J_0$) or $1-x\approx 2K_1<w_0$. Under those conditions, an explicit calculation[35] of the free energies of $\langle\infty\rangle$, $\langle 3\rangle$, and $\langle 4\rangle$ through $O(w_0^2)$ (two flipped spins) shows that $\langle 4\rangle$ acquires a narrow region of stability between $\langle\infty\rangle$ and $\langle 3\rangle$. The obvious next question is whether $\langle 5\rangle$, $\langle 6\rangle$, etc. also appear when there is sufficient anisotropy. This problem is amenable to the same sort of analysis that has been applied here to the $\langle 3\rangle$:$\langle 2\rangle$ pseudoboundary. To treat the $\langle\infty\rangle$:$\langle 3\rangle$ boundary, one

would define a "domain" to be simply the usual ferromagnetic domain (all layers ↑ or all ↓), and the "walls" would then mark the transitions between ↑ and ↓ domains (e.g., . . . ↑↑↑ | ↓↓↓ · · ·). It is then trivially true that all stable phases can be characterized by domain walls separating adjacent domains, so the analysis of I would again apply. At the level of the two-wall interaction $\overline{W}_2(l)$, that analysis would reveal which simple periodic phases $\langle k \rangle$ arise between $\langle \infty \rangle$ and $\langle 3 \rangle$.

At low temperatures, a transfer-matrix method for calculating $\overline{W}_2$ and the other $\overline{W}_n$ could be developed along the lines of this paper. However, if it were desired to exploit the correspondence between the $\overline{W}_n$ and the standard structural coefficients a_ν, as done above, a *new* set of standard structural variables $\{\rho_\nu\}$ would be required, since the set used so far has assumed that all phases are composed of 2 and 3 bands only. [Recall the convention of Sec. II B, leading to (2.17).] By the same token, one cannot immediately decide the stability of $\langle l \rangle$ for small $l \geq 3$ just by appealing to the explicit FS calculations[32] of the free energy through $O(w_0^3)$ (even though a chain of three flipped spins can span a 7 band), since those results also apply only to configurations composed solely of 2 and 3 bands. Therefore, we cannot say more about the $\langle \infty \rangle$:$\langle 3 \rangle$ boundary without first setting up some additional machinery beyond that developed here; but the problem should be soluble by the present methods without any intrinsically new difficulties.

E. Reduced matrix formulation for leading corrections

Because of the second-neighbor range of axial couplings in the ANNNI model, it is not simple to generalize the 4×4 transfer matrix $\mathbf{V}_1$ to arbitrary interlayer coordination numbers, q_1 and q_2. To illustrate the problem, consider the matrix element

$$V_{23}=(\underline{s\hat{s}} \mid \hat{s}\,\hat{s})-(\underline{s\hat{s}} \mid ss \cdots \underline{ss} \mid \hat{s}\,\hat{s}) \; ; \tag{3.65}$$

see Table II. Counting from the left, the first flipped spin may occupy any of the $\frac{1}{2}q_1$ nearest-neighbor positions relative to the second flipped spin which are *also* among the $\frac{1}{2}q_2$ next-nearest-neighbor positions relative to the third flipped spin. The total number of positions available to the first flipped spin therefore depends in a nontrivial way on the lattice structure; moreover, the additional states for which the first flipped spin "sees" the second but not the third, or vice versa, would require that $\mathbf{V}_1$ be enlarged to a matrix larger than 4×4.

This difficulty can be circumvented, however, when only the *leading* correction from extra in-chain flipped spins is really needed in order to resolve the degeneracy at lowest order. In that situation, the crucial point to notice is that, as illustrated in (3.10), one need never consider *three* (or more) *adjacent* layers containing flipped spins, because such a "bound pair of defects," $s \mid \hat{s}\,\hat{s} \mid \hat{s}s \mid$, can always realize an entropic gain by unbinding and separating. The difficulty indicated above can thus be neglected.

Moreover, it follows from this rule that any band in state 3, ($\mid \hat{s}\,\hat{s} \mid$), or state 4, ($\mid \hat{s}s \mid \cdots \mid s\hat{s} \mid$), must be flanked to its left by a state-1 band, $\mid \hat{s}s \mid$, and to its right by a state-2 band, $\mid s\hat{s} \mid$. Equivalently, states 3 and 4 appear only in the products $V_{13}V_{32}$ and $V_{14}V_{42}$. This suggests that one may avoid all explicit reference to states 3 and 4 by working with the *square* of the transfer matrix. More specifically, the results of Secs. III C and III D could equally well have been obtained within the original 2×2 matrix formalism [see (3.13)] that referred only to bands in states 1 and 2, *provided* that the entry $(\mathbf{V}_0^2)_{12}$ of the *square* of the original 2×2 matrix $\mathbf{V}_0$ is changed from its value of 0 in (3.18) to the new value

$$(\mathbf{V}_+^2)_{12} \equiv 2(V_{13}V_{32}+V_{14}V_{42}) \; . \tag{3.66}$$

Here the extra factor of 2 is necessary to allow every 2 band in chain the possibility of being in state 3 or 4: without it, the matrix iteration $(\mathbf{V}_+^2)^{(k+1)/2}$ which gives $\overline{W}_2(l)$ [in the generalization of (3.17)] would have allowed only every *second* 2 band of the chain to be in state 3 or 4.

The matrix elements of (3.26) can be used to evaluate (3.66). The proposed modification of $\mathbf{V}_0^2$ [putting $k=1$ in (3.18)] is then the *augmented* 2×2 matrix

$$\mathbf{V}_+^2 \equiv \begin{bmatrix} \lambda_0^2 & 2\lambda_0^2 x^{2\delta}(1-x^2)w_0 \\ -2\lambda_0 x^{2\delta}(1-x^2) & \lambda_0^2 \end{bmatrix} , \tag{3.67}$$

whose eigenvalues,

$$\lambda_\pm^2=\lambda_0^2[1\pm 2ix^{2\delta}(1-x^2)(w_0/\lambda_0)^{1/2}] \; , \tag{3.68}$$

correctly reproduce the leading terms of the square of $\lambda_\pm$ in (3.43). The rest of the calculation of n-wall interactions $\overline{W}_n$ in Secs. III C and III D may now be carried through alternatively in terms of the eigenvectors of (3.67).

F. Arbitrary coordination numbers and the mean-field limit

The reduced matrix formulation is readily generalized to arbitrary axial coordination numbers q_1, $q_2 \geq 2$. In this general case, one must simply account for all the additional axial bonds between a flipped spin and its unflipped neighbors. The computation of the matrix elements V_{ij} is summarized in a convenient format in Table IV. To illustrate the scheme, recall, from (2.12), that the Boltzmann factor for the broken bond associated with a single pair of axial nearest-neighbor spins flipped from like to unlike orientation is x, while for a pair of axial next-nearest-neighbor spins flipped from *un*like to *like* orientation (the commonest occurrence), the factor is $x^{\kappa'}=x^{q_1\kappa/q_2}$. Reverse transitions are of course associated with the reciprocal factors. Now, any matrix element V_{ij} is associated with a particular configuration of flipped spins according to (3.13) and Table II. Hence,

TABLE IV. Powers of the elementary Boltzmann factors x and $x^{q_1\kappa/q_2}$—corresponding to broken bonds between axial nearest-neighbor and next-nearest-neighbor spins, respectively—that arise in the elements V_{ij} of the augmented 2×2 transfer matrix (3.70) for the ANNNI model with arbitrary axial coordination numbers q_1 and q_2.

Augmented matrix element	Power of x	Power of $x^{q_1\kappa/q_2}$
$V_{11}=(\hat{\underline{s}}\underline{s}\mid\hat{s}s)$	$\frac{1}{2}q_1-\frac{1}{2}q_1=0$	$2(\frac{1}{2}q_2-1)$
$-(\hat{\underline{s}}\underline{s}\mid ss\cdots\underline{ss}\mid\hat{s}s)$	$\frac{1}{2}q_1-\frac{1}{2}q_1=0$	$2\cdot\frac{1}{2}q_2$
$V_{12}=(\hat{\underline{s}}\underline{s}\mid s\hat{s})$	$\frac{1}{2}q_1$	$2\cdot\frac{1}{2}q_2$
$-(\hat{\underline{s}}\underline{s}\mid ss\cdots\underline{ss}\mid s\hat{s})\equiv0$	$\frac{1}{2}q_1$	$2\cdot\frac{1}{2}q_2$
$V_{21}=(s\hat{\underline{s}}\mid\hat{s}s)$	$\frac{1}{2}q_1-2(\frac{1}{2}q_1-1)$	$2\cdot\frac{1}{2}q_2$
$-(s\hat{\underline{s}}\mid ss\cdots\underline{ss}\mid\hat{s}s)$	$\frac{1}{2}q_1-\frac{1}{2}q_1-\frac{1}{2}q_1$	$2\cdot\frac{1}{2}q_2$
$V_{22}=(s\hat{\underline{s}}\mid s\hat{s})$	$\frac{1}{2}q_1-\frac{1}{2}q_1=0$	$2(\frac{1}{2}q_2-1)$
$-(s\hat{\underline{s}}\mid ss\cdots\underline{ss}\mid s\hat{s})$	$\frac{1}{2}q_1-\frac{1}{2}q_1=0$	$2\cdot\frac{1}{2}q_2$
$V_{13}=(\hat{\underline{s}}\underline{s}\mid\hat{s}\hat{s})$	$\frac{1}{2}q_1-\frac{1}{2}q_1=0$	$2(\frac{1}{2}q_2-1)+\frac{1}{2}q_2$
$-(\hat{\underline{s}}\underline{s}\mid ss\cdots\underline{ss}\mid\hat{s}\hat{s})$	$\frac{1}{2}q_1-\frac{1}{2}q_1=0$	$3\cdot\frac{1}{2}q_2$
$V_{32}=(\hat{s}\hat{\underline{s}}\mid s\hat{s})$	$2(\frac{1}{2}q_1-1)-\frac{1}{2}q_1$	$2(\frac{1}{2}q_2-1)+\frac{1}{2}q_2$
$-(\hat{s}\hat{\underline{s}}\mid ss\cdots\underline{ss}\mid s\hat{s})$	$2(\frac{1}{2}q_1-1)-\frac{1}{2}q_1$	$3\cdot\frac{1}{2}q_2$
$V_{14}=(\hat{\underline{s}}\underline{s}\mid\hat{s}s\cdots\underline{ss}\mid s\hat{s})$	$\frac{1}{2}q_1-\frac{1}{2}q_1=0$	$2(\frac{1}{2}q_2-1)+\frac{1}{2}q_2$
$-(\hat{\underline{s}}\underline{s}\mid ss\cdots\underline{ss}\mid\hat{s}s\cdots\underline{ss}\mid s\hat{s})$	$\frac{1}{2}q_1-\frac{1}{2}q_1=0$	$3\cdot\frac{1}{2}q_2$
$V_{42}=-(\hat{\underline{s}}\underline{s}\mid ss\cdots\underline{s\hat{s}}\mid s\hat{s})$	$2\cdot\frac{1}{2}q_1-\frac{1}{2}q_1$	$2(\frac{1}{2}q_2-1)+\frac{1}{2}q_2$
$+(\hat{\underline{s}}\underline{s}\mid ss\cdots\underline{s\hat{s}}\mid ss\cdots\underline{ss}\mid s\hat{s})$	$2\cdot\frac{1}{2}q_1-\frac{1}{2}q_1$	$3\cdot\frac{1}{2}q_2$

the value of V_{ij} is given by the product of these two factors x and $x^{\kappa'}$, raised to powers which are the numbers of the corresponding broken bonds in the associated configuration. These powers are totaled in Table IV. Additionally, each V_{ij} carries a factor given by the number of lattice positions available to the newly flipped spin or spins (which are underlined in Table IV): thus, for example, one obtains

$$V_{11}=\tfrac{1}{2}q_2(x^0x^{\kappa'(q_2-2)}-x^0x^{\kappa'q_2})$$

$$=\tfrac{1}{2}q_2x^{q_1\kappa}(x^{-2\kappa'}-1)\ . \tag{3.69}$$

By evaluating the other V_{ij} in (3.13) and (3.66) in a similar fashion, one arrives at the generalized version of the augmented 2×2 matrix (3.67), namely,

$$\mathbf{V}_+^2=\begin{bmatrix}(\lambda_0^{(q)})^2 & q_1x^{q_1-2}x^{q_1\delta}(1-x^2)w_0(\lambda_0^{(q)})^2\\ -q_1\lambda_0^{(q)}x^{q_1\delta}(1-x^2) & (\lambda_0^{(q)})^2\end{bmatrix}, \tag{3.70}$$

where

$$\lambda_0^{(q)}\equiv\tfrac{1}{2}q_2x^{q_1\kappa}(x^{-2\kappa'}-1),\quad \kappa'=q_1\kappa/q_2\ . \tag{3.71}$$

Observe that $\lambda_0^{(2)}$ is identical to λ_0 as defined in (3.14).

Comparison of this result with (3.67) shows that the form of the transfer matrix is not significantly altered as q_1 and q_2 are varied. In particular, the eigenvalues of $\mathbf{V}_+^2$ always remain complex: explicitly one has

$$\lambda_\pm^2=(\lambda_0^{(q)})^2[1\pm2ic_q(x)(w_0)^{1/2}]\ , \tag{3.72}$$

$$c_q(x)\equiv\tfrac{1}{2}q_1x^{q_1\kappa-1}(1-x^2)(\lambda_0^{(q)})^{-1/2}\ . \tag{3.73}$$

[Compare (3.43) and (3.44).] Consequently, the ANNNI model at fixed low temperature never realizes "devil's last step" behavior. An explicit form for the two-wall interaction, $\overline{W}_2(l)$, is obtained by evaluating the general transfer-matrix expression using $\mathbf{V}_+$ in the basis of eigenvectors of (3.70), using the generalizations to arbitrary q_i of the row and column vectors in (3.15) and (3.16). The result is

$$\overline{W}_2(l)\approx x^{1-q_1\kappa}(1-x^{q_1\kappa})^2(\lambda_0^{(q)})^{k+1/2}w_0^{k+3/2}\sin\left[\left[k+1+\frac{4(1-x^{q_1})\lambda_0^{(q)}}{q_1(1-x^2)(1-x^{q_1\kappa})}\right]c_q(x)(w_0)^{1/2}\right] . \tag{3.74}$$

This shows that the arrangement of $\langle 2^k 3\rangle$ phases remains, for all $q_1, q_2 \geq 2$, qualitatively as depicted in Fig. 4.

These remarks are still valid in the mean-field limit in which $q_i \to \infty$ with $q_i J_i$ $(i=0,1,2)$ held constant. In that limit, $x \to 1$ while κ and

$$x^{q_1}=e^{-2q_1K_1}\equiv x_1 \tag{3.75}$$

remain fixed. [Recall the definitions of Boltzmann factors in (2.3) and (2.12).] Therefore the expressions derived above assume the limiting forms

$$\lambda_0^{(q)}\to\lambda_0^{(\infty)}=2q_2\,|\,K_2\,|\,x_1^{\kappa} , \tag{3.76}$$

$$c_q(x)\to c_\infty(x)=\kappa^{-1}(\lambda_0)^{1/2} , \tag{3.77}$$

whence

$$\overline{W}_2(l)\approx x_1^{-\kappa}(1-x_1^{\kappa})^2(\lambda_0^{(\infty)})^{k+1/2}w_0^{k+3/2}\sin\left[\left[k+1+\frac{2\kappa x_1^{\kappa}(1-x_1)}{(1-x_1^{\kappa})}\right]\frac{(\lambda_0^{(\infty)}w_0)^{1/2}}{\kappa}\right] . \tag{3.78}$$

Contact can again be made with the results of Villain and Gordon[29] by restricting these general mean-field expressions to the "intermediate" temperature range (3.3) in which

$$q_1K_1\to 1, \quad x_1\approx 1-2q_1K_1 . \tag{3.79}$$

In that case, the mean-field two-wall interaction (3.78) becomes

$$\overline{W}_2(l)\approx 2q_2\,|\,K_2\,|\,(2q_2\,|\,K_2\,|\,w_0)^{k+3/2} \times\sin[\kappa^{-1}(k+3)(2q_2\,|\,K_2\,|\,w_0)^{1/2}] , \tag{3.80}$$

which agrees precisely with the corresponding quantity $\beta U_1(2k+3)$ [compare (3.52)] obtained by Villain and Gordon from their harmonic approximation to mean-field theory. (Observe that here, as in all mean-field treatments of the ANNNI model, the coordination numbers q_i always appear only within the products q_iJ_i.)

The three-wall interaction, $\overline{W}_3(l,l)$, can also be calculated for arbitrary q_i from the general transfer-matrix expression (3.21), along the lines of Sec. III D. One first needs to construct the matrix **C** in (3.20) for arbitrary q_i, in order to obtain the generalized version of (3.22), and then equate the coefficients of that result with the expansion in powers of k of a form like (3.53). Depending on the details of the result, it is possible that the interval of values $[k^{(1)}(T),k^{(2)}(T)]$, over which the mixed phases $\langle 2^k 32^{k+1}3\rangle$ are found to be stable when $q_1=q_2=2$ (recall Sec. III D), might be significantly altered or even destroyed. However, the approximate Villain-Gordon result (3.61), for the mean-field form of $\overline{W}_3(l,l)$, suggests that no such profound changes will occur.

IV. CONCLUDING REMARKS

The detailed calculations for the ANNNI model described above provide a fair sampling of the variety of low-temperature behavior discussed in I for systems that exhibit uniaxial arrays of domain walls. Not only has the low-temperature phase diagram of the original model (with $q_1=q_2=2$) been elucidated, but its generalization to arbitrary coordination numbers has also been studied: this has permitted the extraction of asymptotically exact expressions for mean-field theory. Thus, we have demonstrated that there is *no* qualitative disagreement between the ANNNI model and its mean-field limit (contrary to some earlier speculations). Further, we have shown that the harmonic approximation of Villain and Gordon provides a surprisingly accurate account of the mean-field theory. In addition to rederiving previously established results from a more physical and intuitive approach, we have also established the existence of more complicated mixed phases like $\langle 2^k 32^{k+1}3\rangle$, with alternating interwall separations, down to arbitrarily low temperatures.

Our studies have been carried out with the aid of a transfer-matrix formulation for the n-wall interactions W_n. The functional form of these W_n is largely determined by the nature of the transfer-matrix eigenvalues (in particular, whether they be real or complex); that question, in turn, is strongly influenced by the contributions of the *disconnected* configurations of flipped spins, which can drive certain transfer matrix entries negative. This fact leaves us with some reservations concerning the work of Uimin,[39] who ignored all disconnected configurations in utilizing an FS type of expansion to study the ANNNI model in nonzero magnetic field. To illustrate the danger within the context of the *zero-field* calculations performed here, consider the effect of omitting the negative term due to disconnected configurations in each transfer-matrix entry V_{ij}. In the simplest case $q_1=q_2=2$ (which Uimin studied), the augmented 2×2 matrix in (3.67) would become

$$\mathbf{V}_+^2=\begin{bmatrix} 1 & 2x^{2\delta}w_0 \\ 2x^{2\kappa+1} & 1 \end{bmatrix} , \tag{4.1}$$

which has *real* eigenvalues. Such a shift from complex

to real eigenvalues might also, depending on the sign of the resulting amplitudes in the spectral representation of $W_2(l)$, induce a change in the two-wall interaction from case B ("harmless staircase") to case A ("devil's last step") behavior. (For the zero-field example just given, the reader may check that $W_2(l)$ actually remains within case B, although, of course, it is no longer oscillatory!) Consequently, it is possible that some or all of the devil's staircase behavior reported by Uimin is spurious, arising from his neglect of disconnected configurations.

That is one of several remaining open questions that may be answerable within the scope of the transfer-matrix approach utilized here. Others include, of course, the nature of the higher-order mixed phases that may be present in the ANNNI phase diagram: whether these continue to appear, forming a complete devil's staircase, or are eventually cut off beyond some maximum order. The question of which additional phases arise on the $\langle \infty \rangle$:$\langle 3 \rangle$ pseudoboundary of the ANNNI model for sufficiently anisotropic couplings also remains to be answered. (Recall the discussion at the end of Sec. III D.)

ACKNOWLEDGMENTS

We have benefited from conversations and correspondence with Walter Selke and Jacques Villain. The support of the National Science Foundation, principally through the Materials Science Center at Cornell University but in part through the Condensed Matter Theory Program,[40] is gratefully acknowledged.

---

*Present address: Institute for Physical Science and Technology, University of Maryland, College Park, MD 20742.

†Present address: Department of Physics, University of Utah, Salt Lake City, UT 84112.

[1]M. E. Fisher and A. M. Szpilka, Phys. Rev. B **36**, 644 (1987).

[2]A. M. Szpilka and M. E. Fisher, following paper, Phys. Rev. B **36**, 5363 (1987).

[3]A. M. Szpilka and M. E. Fisher, Phys. Rev. Lett. **57**, 1044 (1986).

[4]R. J. Elliott, Phys. Rev. **124**, 346 (1961).

[5]A. Yoshimori, J. Phys. Soc. Jpn. **14**, 807 (1959).

[6]J. Villain, J. Phys. Chem. Solids **11**, 303 (1959).

[7]U. Enz, Physica (Utrecht) **26**, 698 (1960).

[8]A. Herpin, P. Meriel, and J. Villain, J. Phys. (Paris) **21**, 67 (1960).

[9]K. Yosida and H. Miwa, J. Appl. Phys. **32**, 8S (1961).

[10]Y. Yamada and N. Hamaya, J. Phys. Soc. Jpn. **52**, 3466 (1983).

[11]J. M. Yeomans and G. D. Price, Bull. Mineral. **109**, 3 (1986).

[12]D. de Fontaine and J. Kulik, Acta Metall. **33**, 145 (1985).

[13]P. Ruján, W. Selke, and G. V. Uimin, Z. Phys. B **53**, 221 (1983).

[14]B. Widom, J. Chem. Phys. **84**, 6943 (1986).

[15]P. Bak, Rep. Prog. Phys. **45**, 587 (1982).

[16]W. Selke, in *Modulated Structure Materials,* edited by T. Tsakalakos (Nijhoff, Boston, 1984).

[17]J. M. Yeomans, Solid State Phys. (to be published); see also A. M. Szpilka, Ph.D. thesis, Cornell University, 1985.

[18]W. Selke and M. E. Fisher, Phys. Rev. B **20**, 257 (1979).

[19]W. Selke and M. E. Fisher, J. Magn. Magn. Mater. **15-18**, 403 (1980).

[20]E. B. Rasmussen and S. J. Knak Jensen, Phys. Rev. B **24**, 2744 (1981).

[21]J. von Boehm and P. Bak, Phys. Rev. Lett. **42**, 122 (1979).

[22]C. S. O. Yokoi, M. D. Coutinho-Filho, and S. R. Salinas, Phys. Rev. B **24**, 4047 (1981).

[23]H. C. Öttinger, J. Phys. A **16**, 1483 (1983).

[24]P. M. Duxbury and W. Selke, J. Phys. A **16**, L741 (1983).

[25]W. Selke and P. M. Duxbury, Z. Phys. B **57**, 49 (1984).

[26]M. Høgh Jensen and P. Bak, Phys. Rev. B **27**, 6853 (1983).

[27]P. Bak and J. von Boehm, J. Appl. Phys. **50**, 7409 (1979).

[28]P. Bak and J. von Boehm, Phys. Rev. B **21**, 5297 (1980).

[29]J. Villain and M. B. Gordon, J. Phys. C **13**, 3117 (1980).

[30]M. E. Fisher and W. Selke, Phys. Rev. Lett. **44**, 1502 (1980).

[31]M. E. Fisher, J. Appl. Phys. **52**, 2014 (1981).

[32]M. E. Fisher and W. Selke, Philos. Trans. R. Soc. London Sect. A **302**, 1 (1981).

[33]See also J. Villain, in *Modern Trends in Solid State Theory* (Karl Marx University, Leipzig, 1980).

[34]S. Redner, J. Stat. Phys. **25**, 15 (1981).

[35]This observation was pointed out by D. A. Huse (private communication).

[36]Fisher and Selke denoted the structural variables by l_k instead of ρ_k, but we adopt the latter notation here to avoid confusion with the interwall separations l_i.

[37]Note that this convention differs from that of Fisher and Selke (Ref. 32).

[38]*Handbook of Mathematical Functions,* edited by M. Abramowitz and I. A. Stegun (Dover, New York, 1965).

[39]G. V. Uimin, J. Stat. Phys. **34**, 1 (1984).

[40]Through Grant No. DMR 87-01223.